TECHNICAL MEMORANDUM

X-573

LOW-SPEED AERODYNAMIC CHARACTERISTICS OF A MODEL OF THE DS-1 GLIDER

By Clyde Q. Allen

Ames Research Center
Moffett Field, Calif.

NATIONAL AERONAUTICS AND SPACE ADMINISTRATION

WASHINGTON

August 1961

NATIONAL AERONAUTICS AND SPACE ADMINISTRATION

TECHNICAL MEMORANDUM X-573

LOW-SPEED AERODYNAMIC CHARACTERISTICS OF A MODEL OF THE DS-1 GLIDER*

By Clyde Q. Allen

SUMMARY

The model was tested at Mach numbers of 0.26 and 0.50 and at Reynolds numbers from 5 to 24 million based on the mean aerodynamic chord. The delta-wing glider had 73° of sweep and the configurations included five different body shapes, four vertical tail arrangements, and two sizes each of wing leading-edge radii, elevons, and wing-tip extensions.

Results showing the static longitudinal and lateral-directional aerodynamic characteristics are presented without analysis.

INTRODUCTION

The results presented herein were obtained in the Ames 12-Foot Pressure Wind Tunnel as part of the NASA program supporting the Dyna Soar Project of the United States Air Force. A 0.15-scale model of the DS-1 re-entry glider was supplied by the Boeing Airplane Company. Several configurations of this delta-wing glider were tested at Mach numbers of 0.26 and 0.50 to evaluate the low-speed longitudinal and lateral-directional characteristics. The glider configurations included five different body shapes, four vertical tail arrangements, and two sizes each of wing leading-edge radii, elevons, and wing-tip extensions. The angle-of-attack range was from -4° to +25°, and the angle-of-sideslip range was from -4° to +16°. The Reynolds numbers ranged from 5 to 24 million based on the wing mean aerodynamic chord. The majority of the configurations were tested at a Mach number of 0.26 and at a Reynolds number of either 5 or 15 million. To expedite publication, the data are presented without analysis.

*Title, Unclassified

[redacted]

COEFFICIENTS AND SYMBOLS

The measured force and moment coefficients presented in this report are referenced to the body-axis system, except the lift and drag coefficients which are referenced to the wind-axis system (see fig. 1). The moments for all configurations are referred to a point 3.152 feet aft of the vertex obtained by extending the leading edges, and 3.75 inches above the bottom surface of the wing. For all configurations except those involving the E_2 elevons, this moment center is at 43.73 percent $\bar{c}$. For configurations involving the E_2 elevons, the moment center is at 38.34 percent $\bar{c}$.

b span, 2.883 ft (19.22 ft, full scale)

$\bar{c}$ mean aerodynamic chord, 3.098 ft (for W_1E_1)(20.65 ft, full scale); 3.167 ft (for W_1E_2)(21.11 ft, full scale)

C_L lift coefficient, $\frac{\text{lift}}{qS}$

C_m pitching-moment coefficient, $\frac{\text{pitching moment}}{qS\bar{c}}$

C_D drag coefficient, $\frac{\text{drag}}{qS}$

C_Y side-force coefficient, $\frac{\text{lateral force}}{qS}$

C_n yawing-moment coefficient, $\frac{\text{yawing moment}}{qSb}$

C_l rolling-moment coefficient, $\frac{\text{rolling moment}}{qSb}$

C_{p_b} base-pressure coefficient, $\frac{p_b - p}{q}$

M free-stream Mach number

p_b base pressure

p free-stream static pressure

q free-stream dynamic pressure

R Reynolds number based on wing mean aerodynamic chord, 3.098 ft

S wing area, 7.486 sq ft (for W_1E_1)(332.7 sq ft, full scale); 8.139 sq ft (for W_1E_2)(361.7 sq ft, full scale)

[redacted]

α angle of attack (referred to bottom surface of wing) corrected for tunnel-wall interference, deg

α_u geometric angle of attack (referred to bottom surface of wing), deg

α_T incidence of tip extensions (measured between the wing-tip-extension chord and the bottom surface of wing)(negative deflection - tip-extension trailing edge up), deg

β angle of sideslip, deg

δ_e elevon deflection (measured between the bottom surfaces of wing and elevon)(negative deflection - elevon trailing edge up), deg

The following symbols are used in this report to describe the glider configurations and will identify the component parts of each configuration.

W_1 73° swept wing

L_1 standard wing leading edge (4-in. lower radius, 2-in. upper radius, full scale)

L_2 modified wing leading edge (4-in. lower radius, 6-in. upper radius, full scale)

B_1 standard body

B_2 cone-cylinder body

B_3 B_1 body with extension (used only with E_2 elevons)

B_4 flat-nosed body (see fig. 5(a))

V_1 standard vertical tails, 8° toe-in (31 sq ft each, full scale)

V_2 large vertical tails, tilted out 20° (43 sq ft each, full scale)

V_3 large vertical tails, not tilted out (43 sq ft each, full scale)

V_4 standard vertical tails, 4° toe-in (31 sq ft each, full scale)

E_1 standard elevons (small elevons; total area, 45 sq ft, full scale)

E_2 large elevons (total area, 68.2 sq ft, full scale)

T_1 large wing-tip extension (low aspect ratio; total area, 22.98 sq ft, full scale)

T_2 small wing tip extension (high aspect ratio; total area, 11.9 sq ft, full scale)

X_1 body fillet

MODEL

The 0.15-scale model was supplied by the Boeing Airplane Company. The model had a modified delta plan-form wing with 73° sweep and a fuselage mounted on the upper surface of the wing. The wing and control surfaces were made of aluminum and the bodies were fabricated from aluminum, wood, and impregnated glass fiber. The components used for the various modifications are listed under the section Coefficients and Symbols and the principal model dimensions are given in figure 2. Photographs of some of the model configurations are presented in figures 3 through 7. The model was supported by an internal six-component strain-gage balance and was sting mounted in the wind-tunnel test section. The elevons were actuated by electric motors which permitted remote control of the deflection angles.

A 5 2 3

Seven orifices were used to survey the model base pressures on the standard $W_1L_1B_1V_1E_1$ configuration only. These orifices were distributed across the trailing edges of the left vertical tail and elevon, and across the left side of the body base, and were connected to a multiple-tube manometer. A single orifice was secured to the sting inside the model cavity just forward of the base.

TESTS

Six-component force and moment measurements were made in the Ames 12-Foot Pressure Wind Tunnel to determine the longitudinal and lateral-directional characteristics of the model configurations over an angle-of-attack range from -4° to +25° and sideslip range from -4° to +16°, the latter at constant angle of attack of either 0°, 6°, or 9°. The free-stream Mach number for most of the experiments was 0.26 and the Reynolds number was either 5 million or 15 million. Some data were obtained for a Mach number of 0.26 and a range of Reynolds numbers from 5 million to 24 million. In addition, measurements were also made for a Mach number of 0.50 and a Reynolds number of 9 million.

The elevons were deflected together as longitudinal controls or differentially as roll controls, and the limits of deflection were +15° and -20°. The deflections of the wing-tip extensions were limited to 0° and -10°.

Experiments were made at two Reynolds numbers with artificial roughness on the standard glider configuration to insure a completely turbulent boundary layer. The roughness was applied as strips of No. 60 and No. 100 carborundum grains along the wing leading edges.

Pressure measurements were made for two Reynolds numbers for the standard glider configuration at seven points distributed across the left side of the base and at a single point located within the model balance cavity.

REDUCTION OF DATA

The data have been corrected for the induced effects of the tunnel walls resulting from lift on the model by the method of reference 1. The magnitudes of the corrections which were added to the measured values are:

$$\Delta\alpha = 0.52\ C_L$$

$$\Delta C_D = 0.0091\ C_L^2$$

Corrections to the data to account for the effects of constriction due to the tunnel walls were calculated by the method of reference 2, and angles of attack and sideslip have been corrected for the deflection of the sting support system under load. The effect of interference between the model and sting support is not known.

The plan-form areas of the two types of elevons, E_1 and E_2, were included in the wing area appropriate to each configuration. Hence, two values for both wing area and mean aerodynamic chord are listed in the Coefficients and Symbols section. For configurations without the elevons, the wing area used for calculating the force and moment coefficients included the area of the small elevons, E_1. It should be noted that for configurations with wing-tip extensions, the wing area was not adjusted to include the areas of the tip extensions. Drag data are presented as measured without adjustments for base pressure.

RESULTS

The results of the wind-tunnel investigation of the DS-1 glider and modifications are presented in figures 8 through 29 as follows:

A 5 2 3

It should be noted that for the majority of the results, the scale of the pitching-moment coefficients is 0.01 per inch. This expanded scale was used to make the effects of configuration modifications more apparent than would have been the case if the pitching-moment coefficients had been plotted to the more conventional scale of 0.04 per inch used in figures 17, 18, and 19.

Ames Research Center
National Aeronautics and Space Administration
Moffett Field, Calif., May 12, 1961

REFERENCES

1. Glauert, H.: The Elements of Aerofoil and Airscrew Theory. Ch. XIV, The University Press, Cambridge, England, 1926.

2. Herriot, John G.: Blockage Corrections for Three-Dimensional-Flow Closed-Throat Wind Tunnels, With Consideration for the Effect of Compressibility. NACA Rep. 995, 1950. (Supersedes NACA RM A7B28)

[redacted]

A
5
2
3

[redacted]

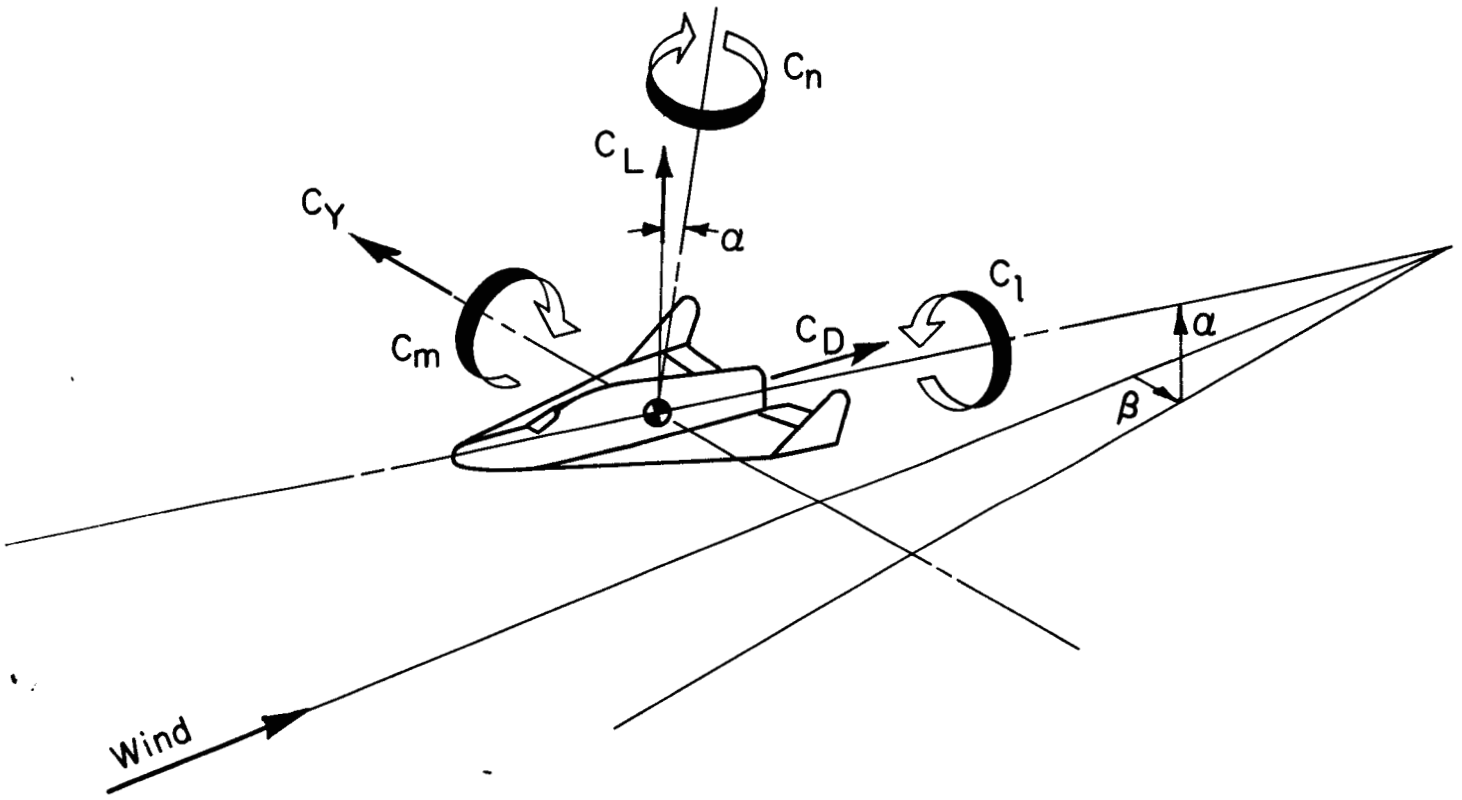

Figure 1.- The sign convention used in presentation of the data. Positive directions of force and moment coefficients are shown.

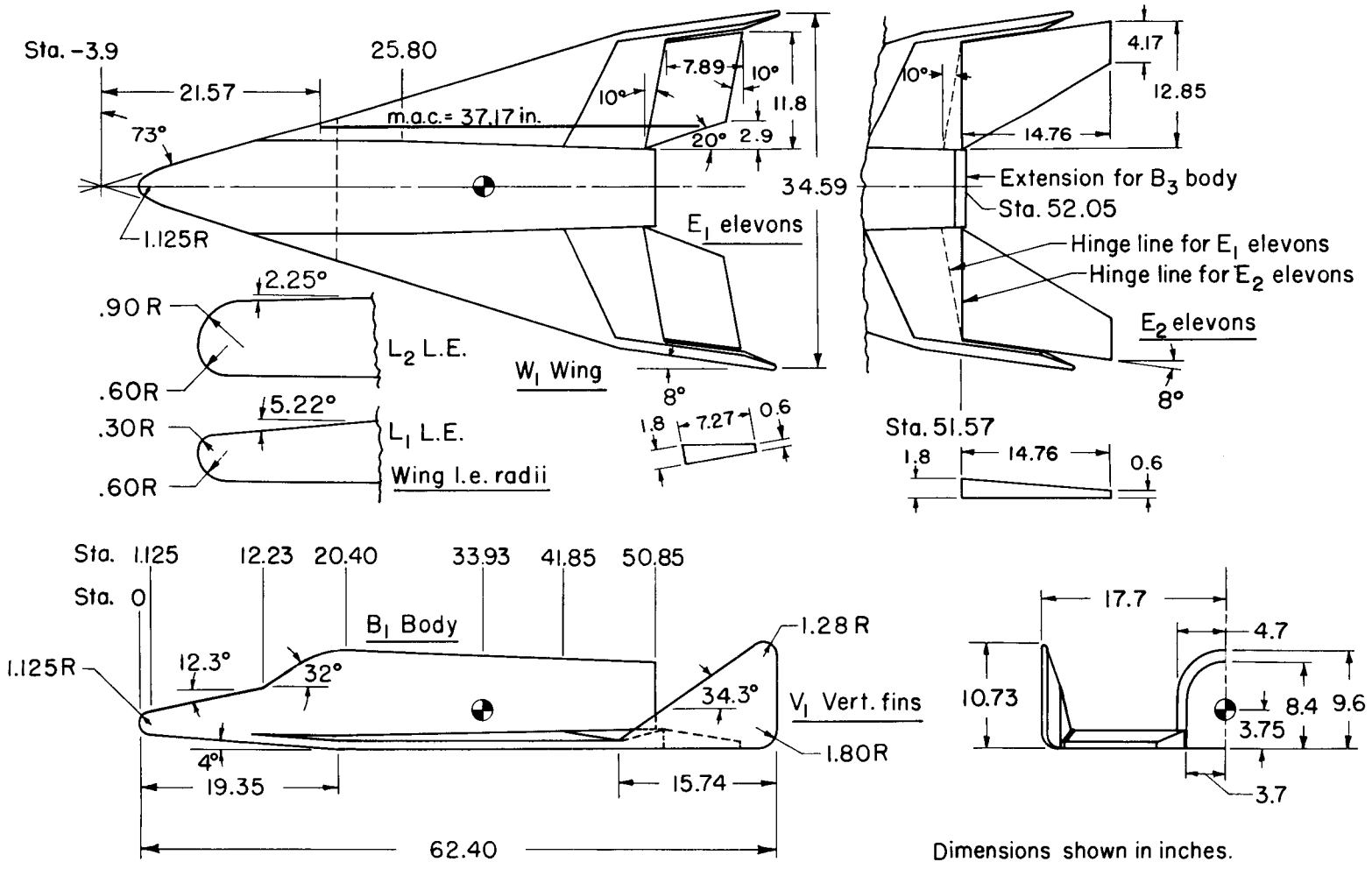

(a) Dimensions of the standard configuration, and details of modifications to the wing leading edges and the elevons.

Figure 2.- Sketches of the model and modifications.

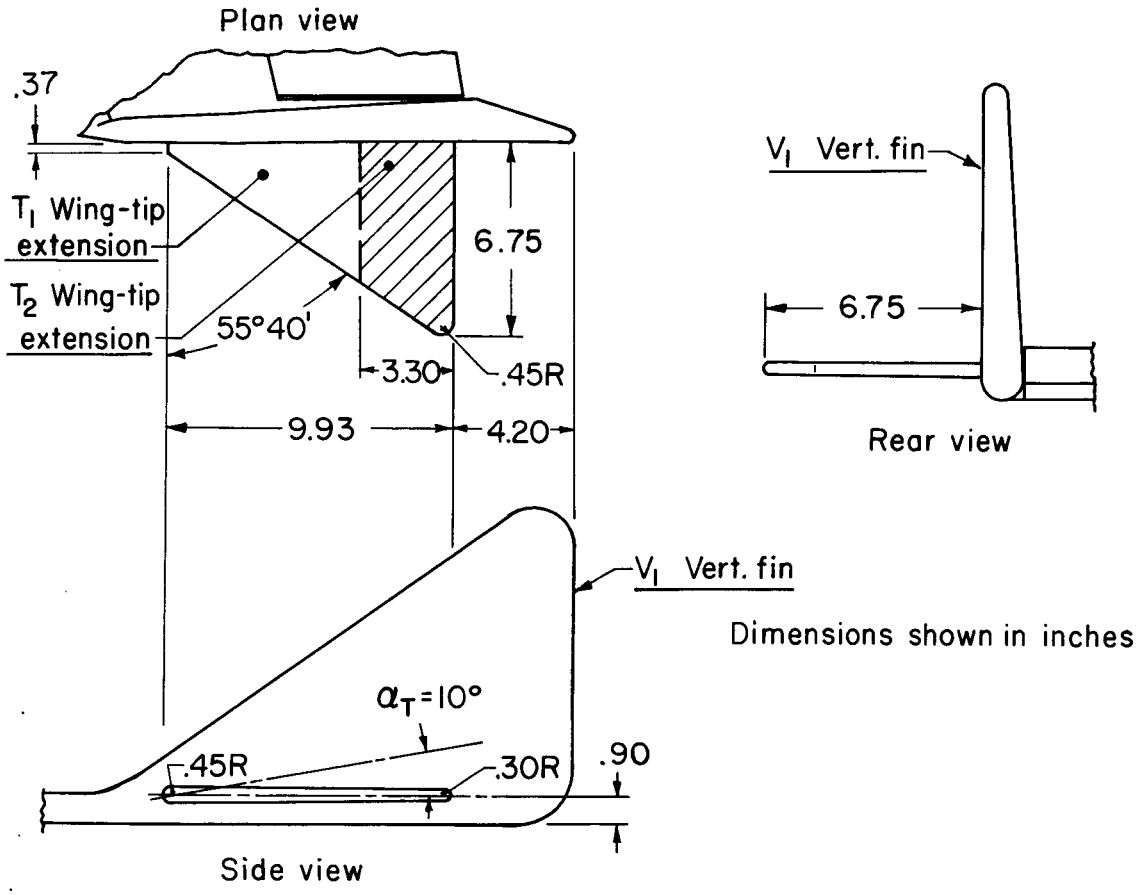

(b) Wing-tip extensions.

Figure 2.- Continued.

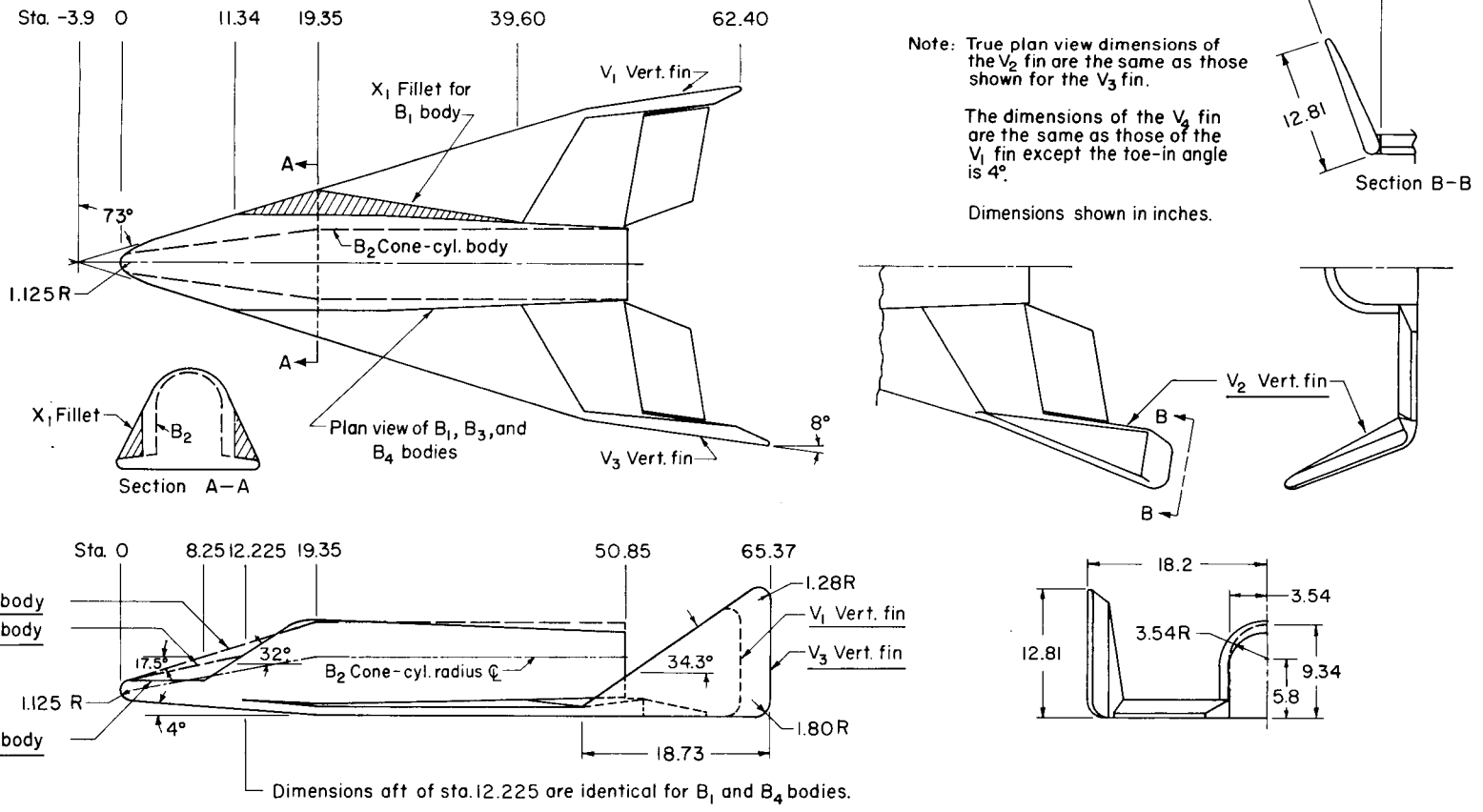

(c) Body and vertical fin modifications.

Figure 2.- Concluded.

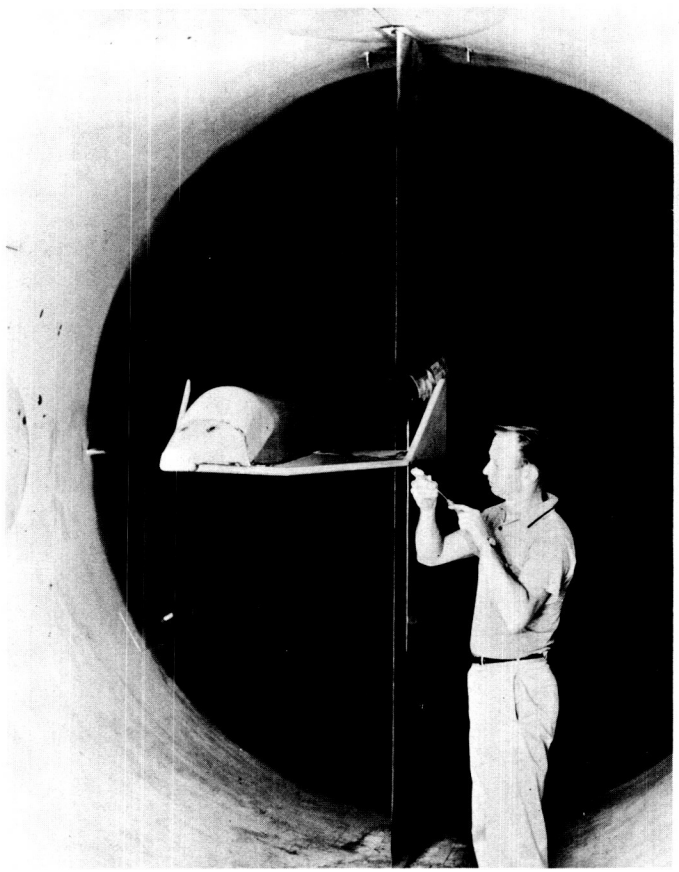

A-27074

(a) $\alpha = -1^{\circ}$.

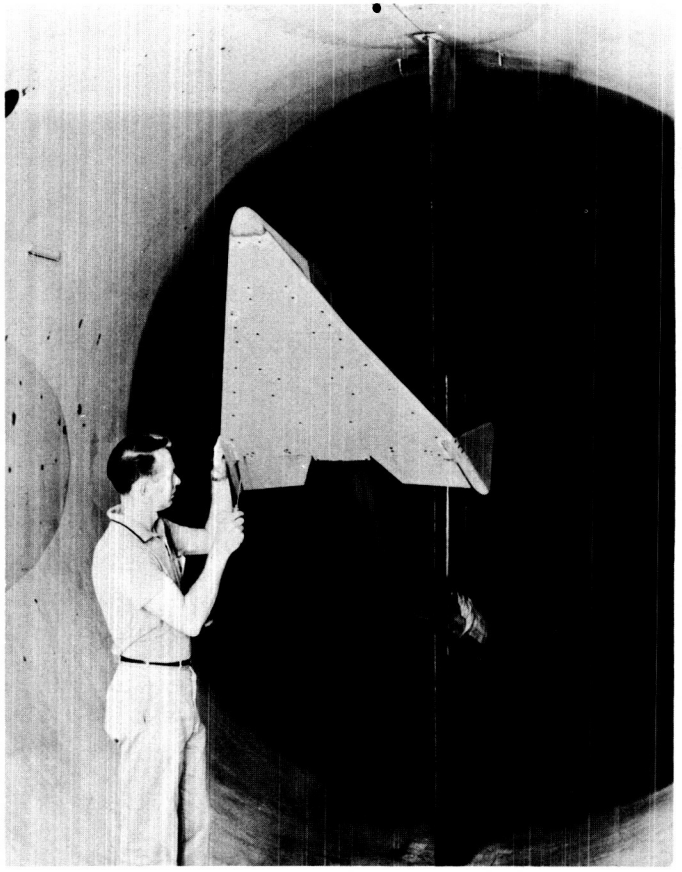

A-27075

(b) $\alpha = 26^{\circ}$.

Figure 3.- Photographs of the model with the standard configuration in the wind tunnel ($W_1L_1B_1V_1E_1$).

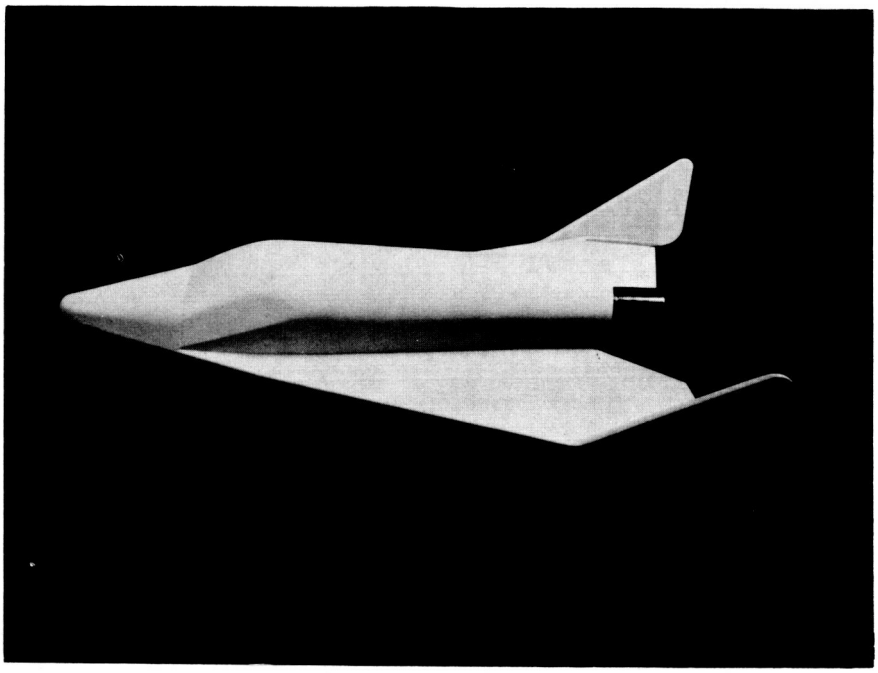

A-27076

(c) Side view.

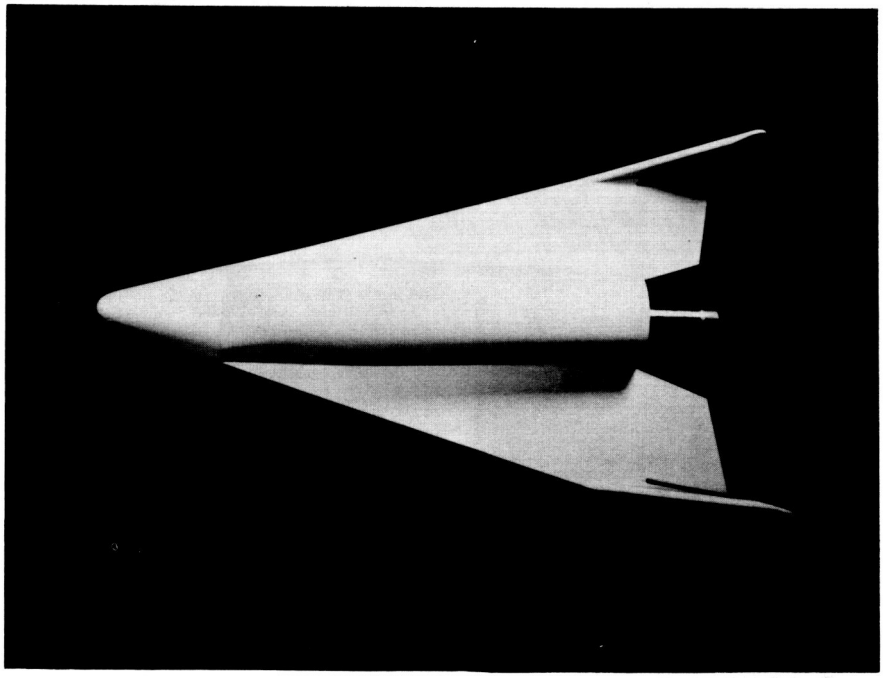

A-27077

(d) Top view.

Figure 3.- Concluded.

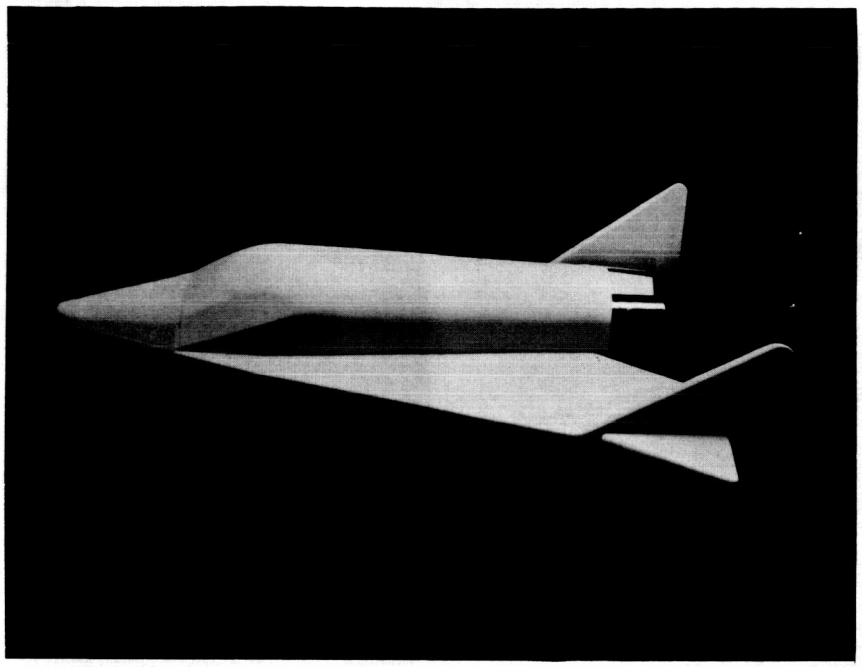

A-27078

(a) Side view; large wing-tip extension T_1; $\alpha_T = -10^\circ$.

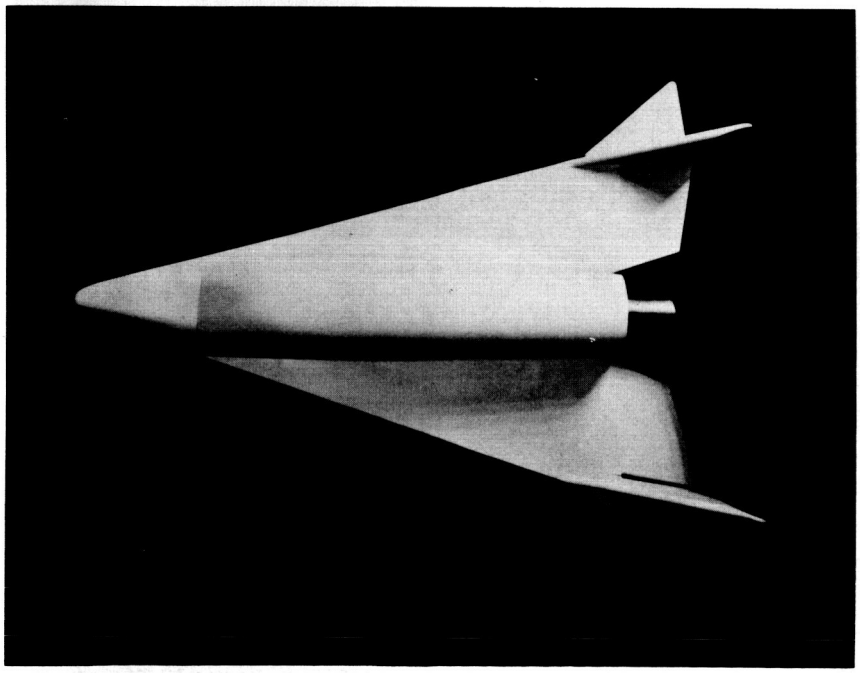

A-27079

(b) Top view; large wing-tip extension T_1; $\alpha_T = -10^\circ$.

Figure 4.- Photographs of the model with wing-tip extensions.

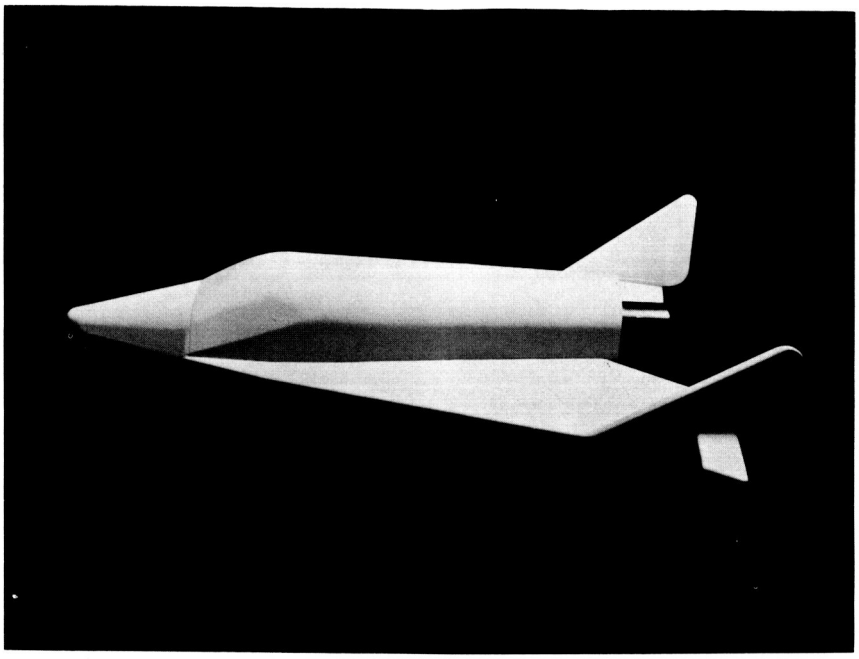

A-27080

(c) Side view; small wing-tip extension T_2; $\alpha_T = -10^\circ$.

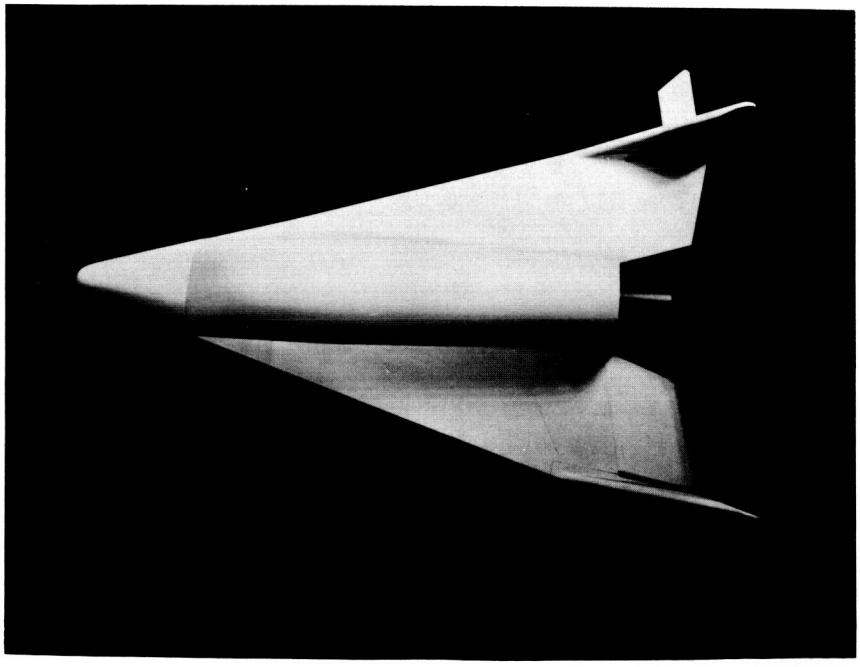

A-27081

(d) Top view; small wing-tip extension T_2; $\alpha_T = -10^\circ$.

Figure 4.- Concluded.

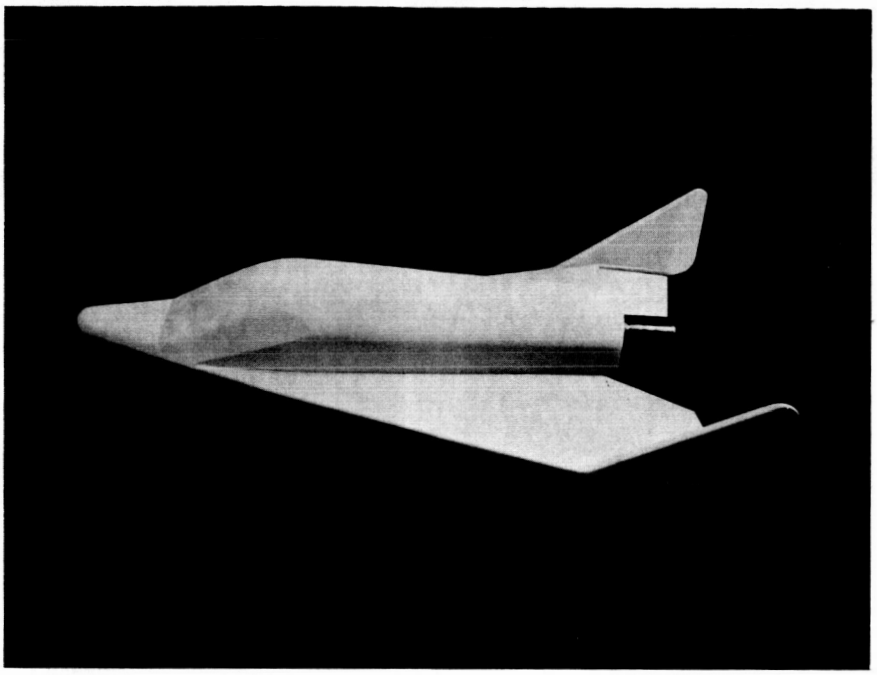

A-27082

(a) Flat nosed body ($W_1L_1B_4V_1E_1$).

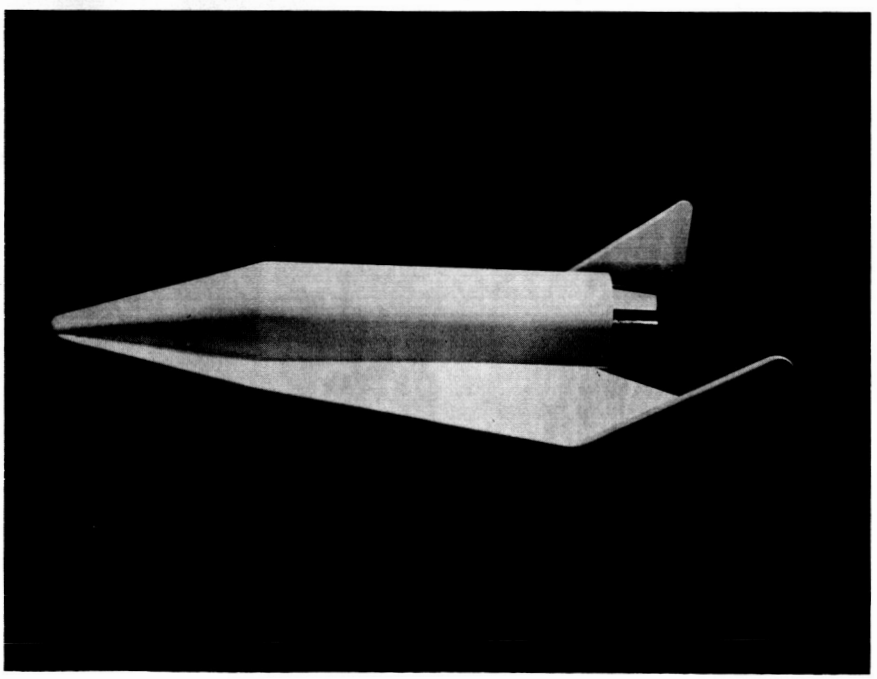

A-27083

(b) Cone-cylinder body ($W_1L_1B_2V_1E_1$).

Figure 5.- Photographs of the model with body modifications.

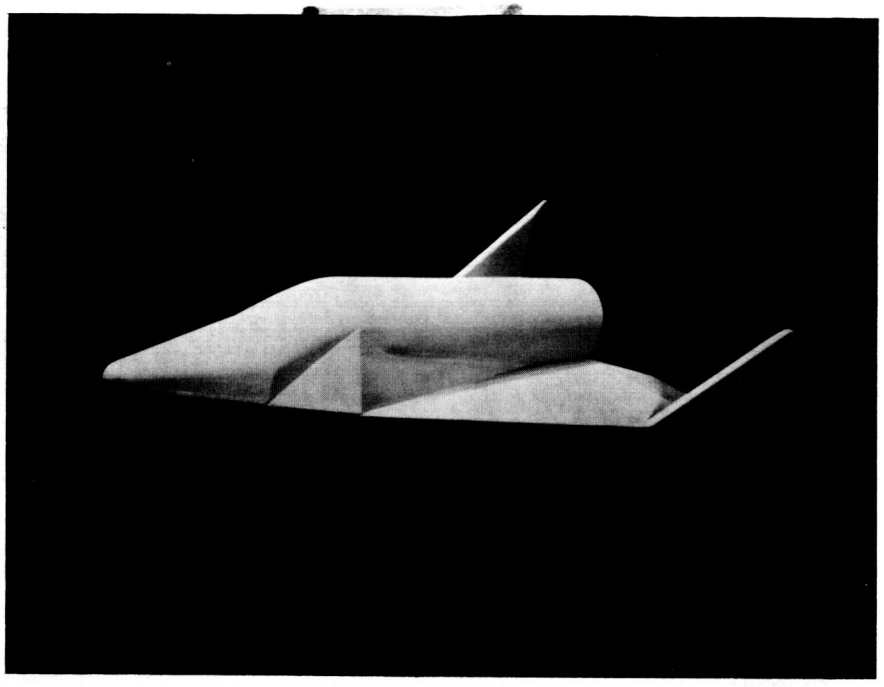

A-27084

(c) Standard body with fillet ($W_1L_1B_1V_1E_1X_1$).

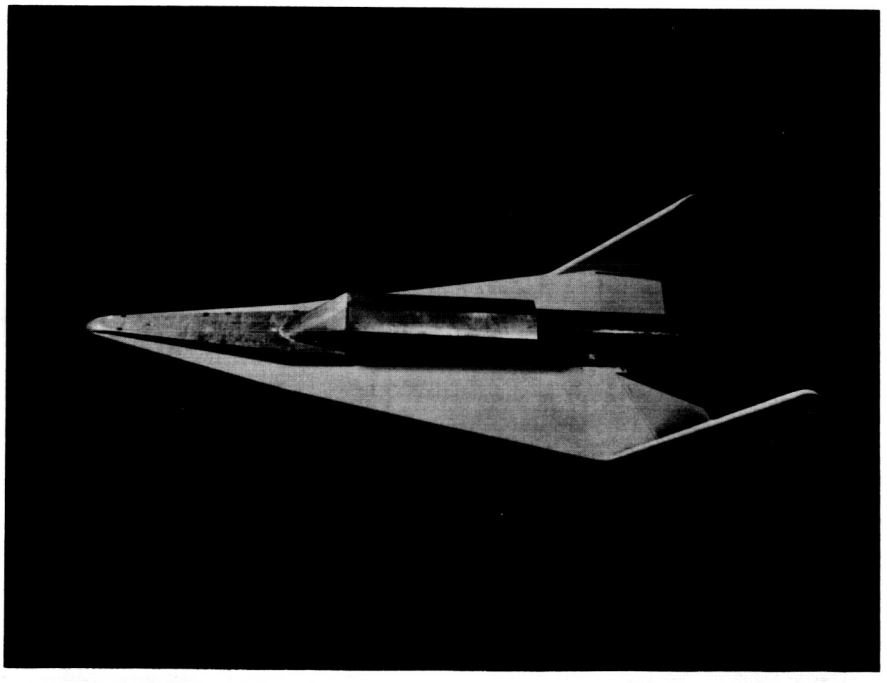

A-27088

(d) Model with the body removed ($W_1L_1V_1E_1$).

Figure 5.- Concluded.

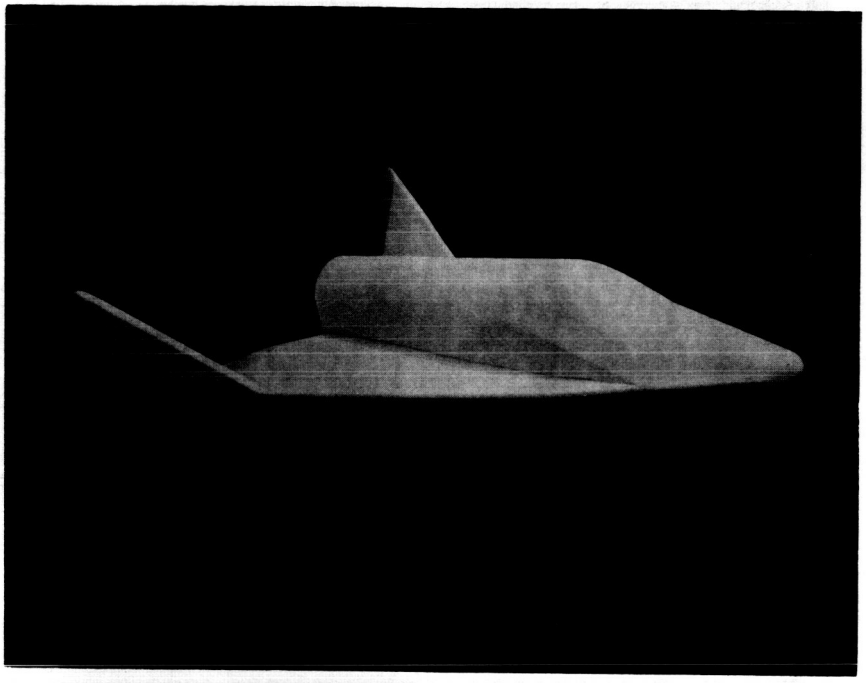

(a) Three-quarter front view.

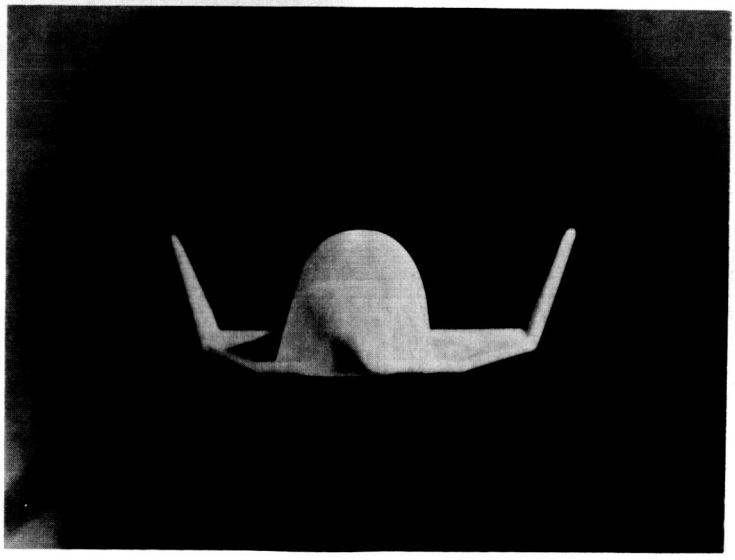

(b) Front view.

Figure 6.- Photographs of the model with the large vertical tails tilted out 20° ($W_1L_1B_1V_2E_1$).

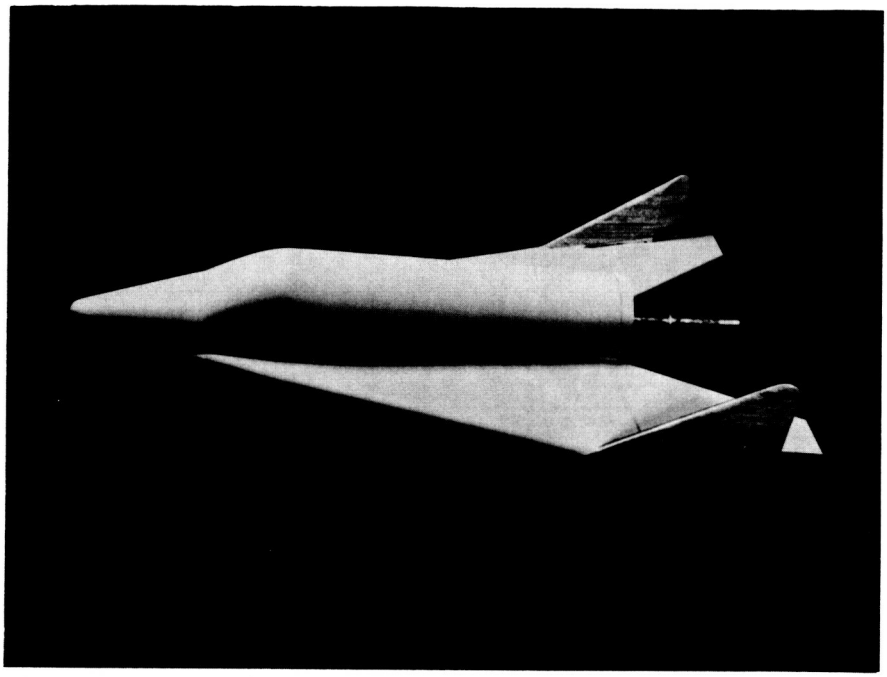

A-27087

Figure 7.- Photograph of the model with the modified wing leading edge, extended body, vertical tails with reduced toe-in, and large elevons ($W_1L_2B_3V_4E_2$).

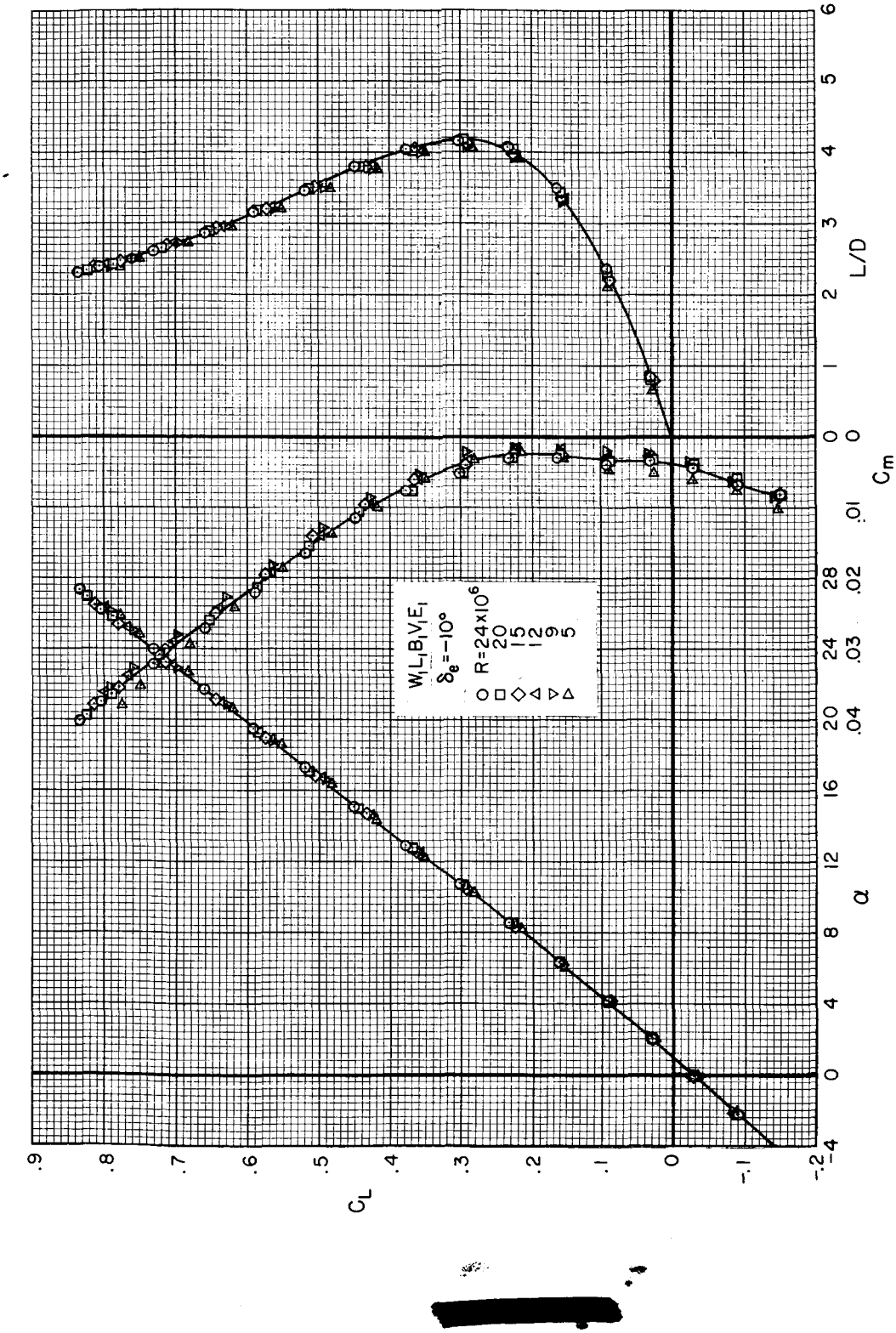

Figure 8.- The effects of Reynolds number on the longitudinal characteristics; $\beta = 0°$, M = 0.26.

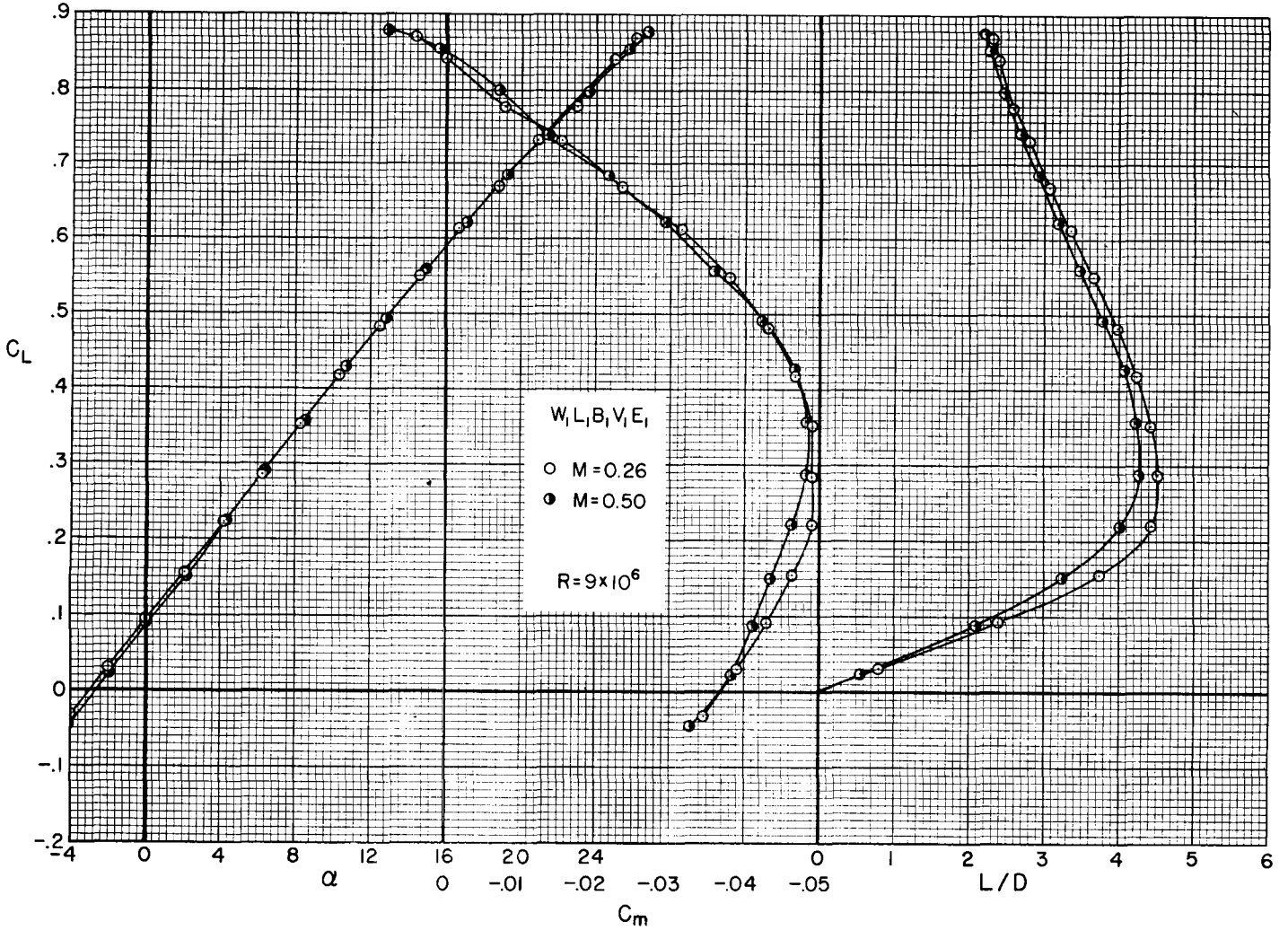

(a) $\delta_e = 0^\circ$

Figure 9.- A comparison of the longitudinal characteristics for two Mach numbers; $\beta = 0^\circ$.

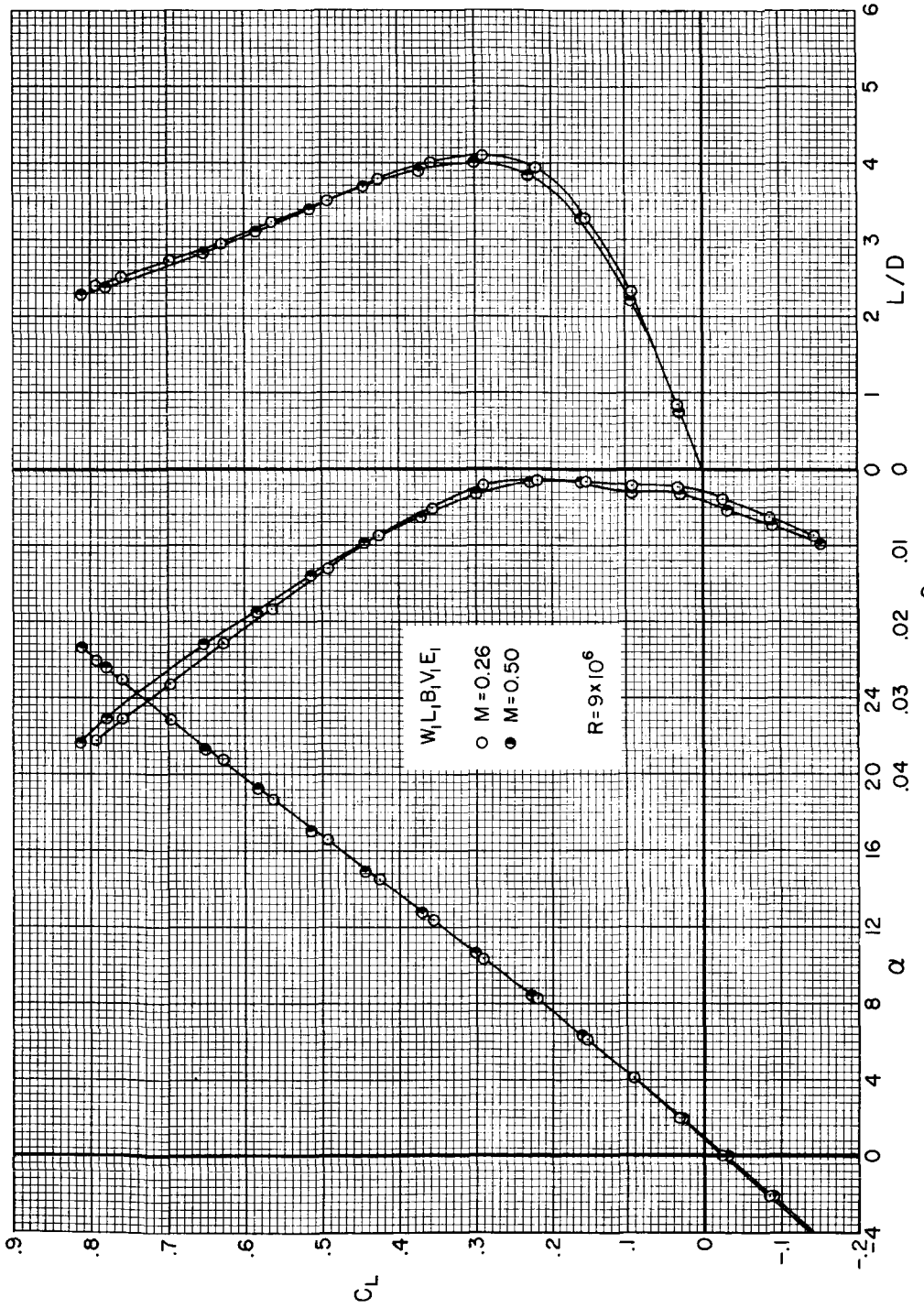

(b) $\delta_e = -10^\circ$

Figure 9.- Concluded.

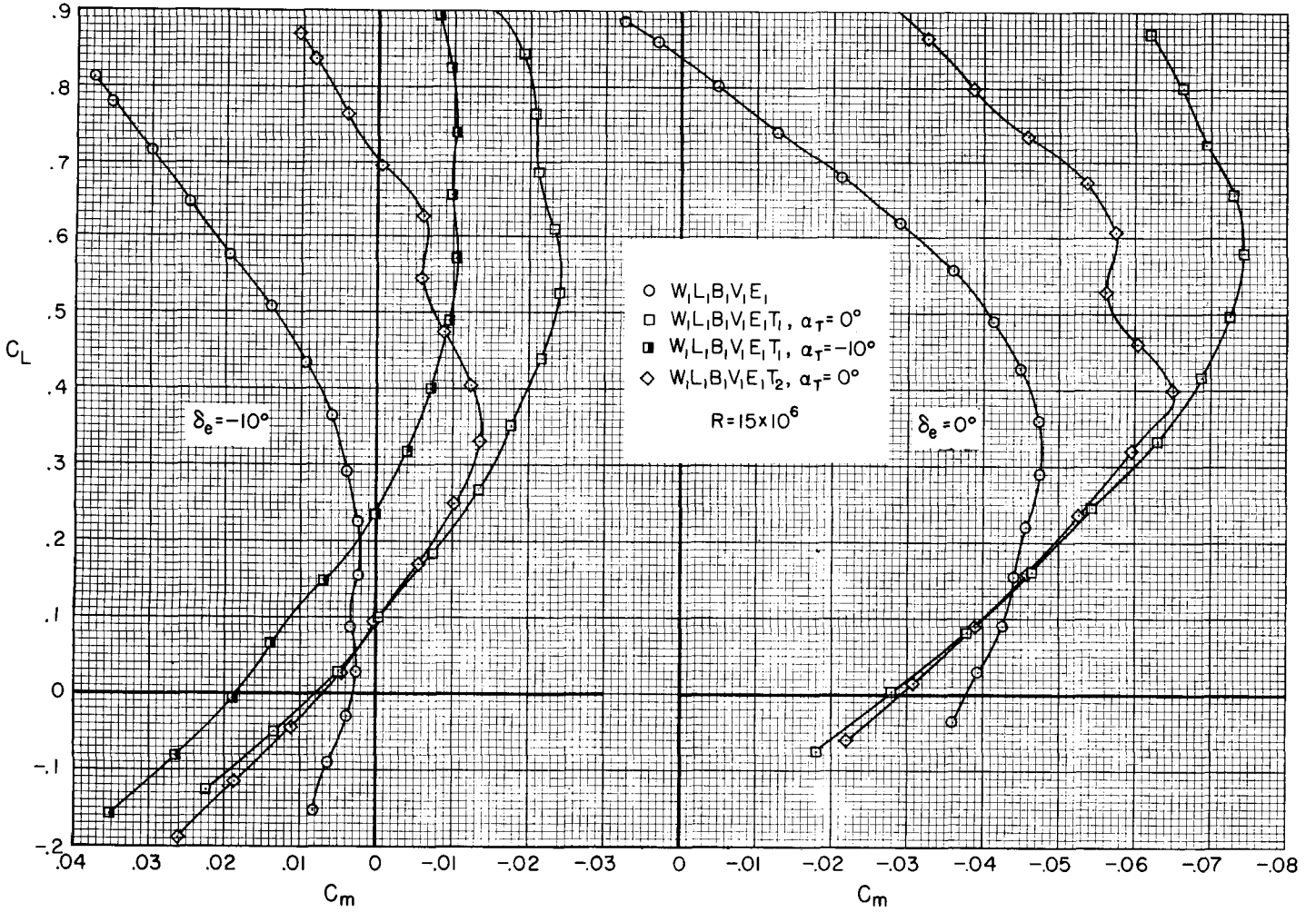

(a) C_L vs. C_m

Figure 10.- The effects of wing-tip extensions on the longitudinal characteristics; $\beta = 0°$, $M = 0.26$.

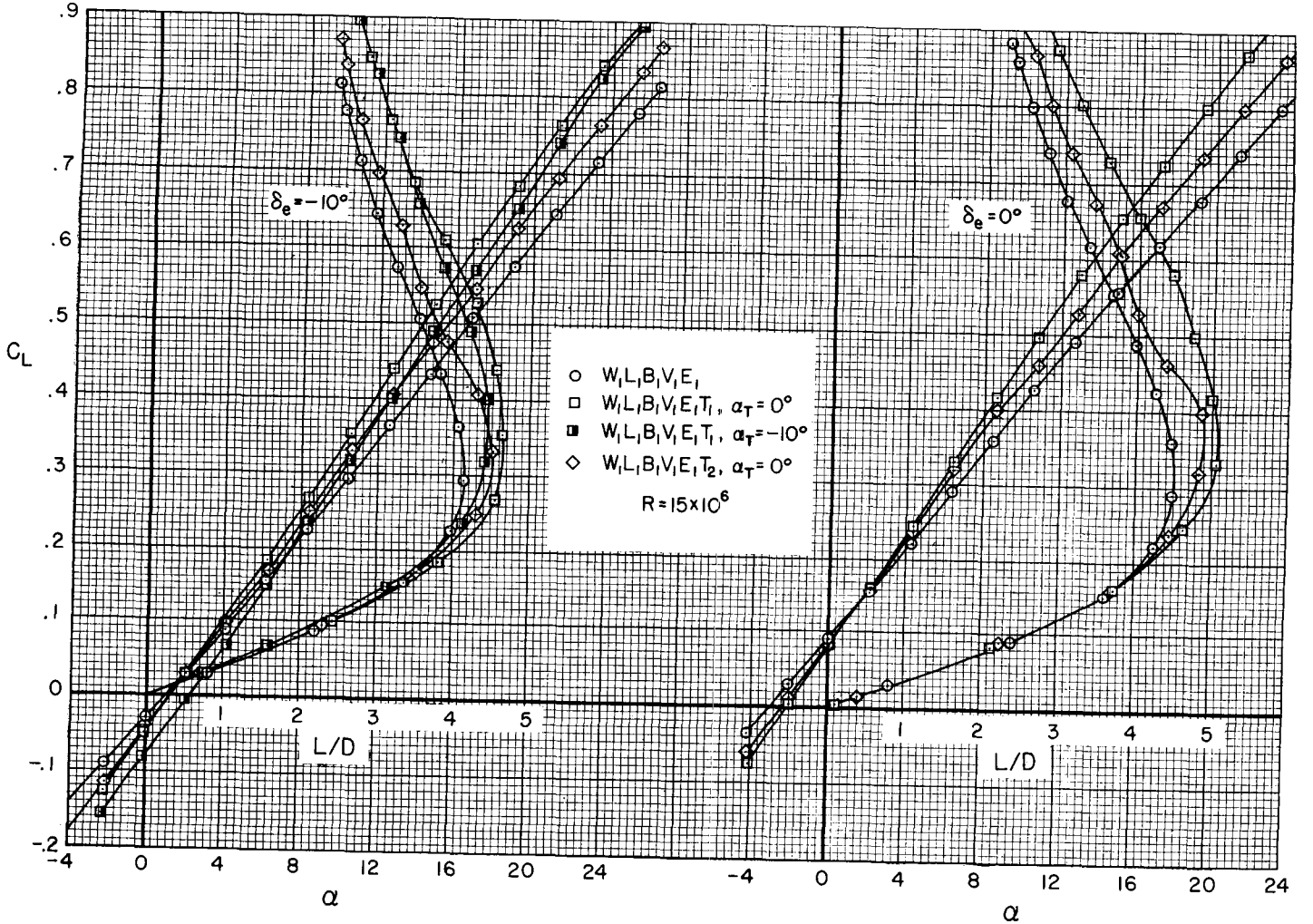

(b) C_L vs. α and C_L vs. L/D

Figure 10.- Concluded.

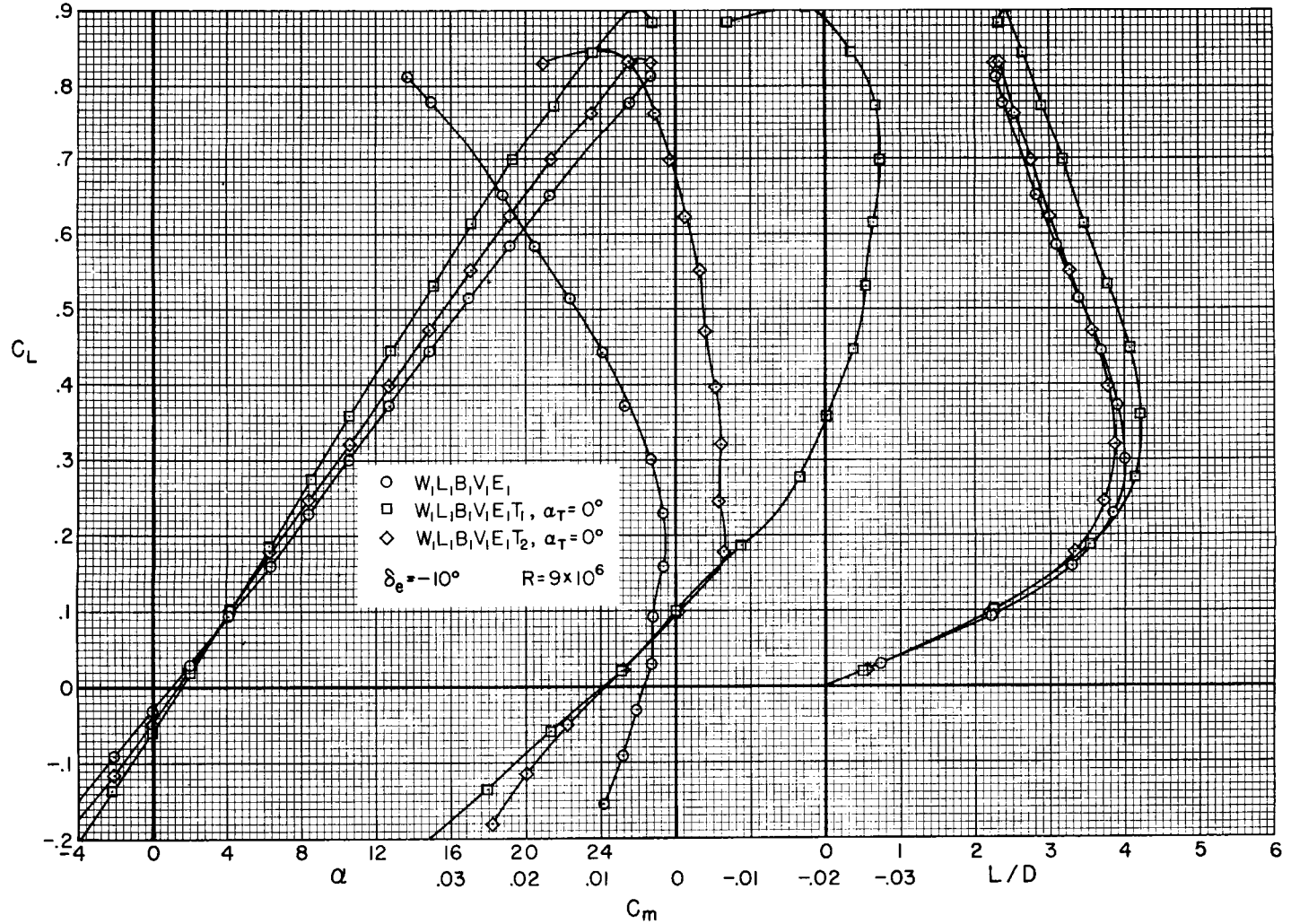

Figure 11.- The effects of wing-tip extensions on the longitudinal characteristics; $\beta = 0^o$, $M = 0.50$.

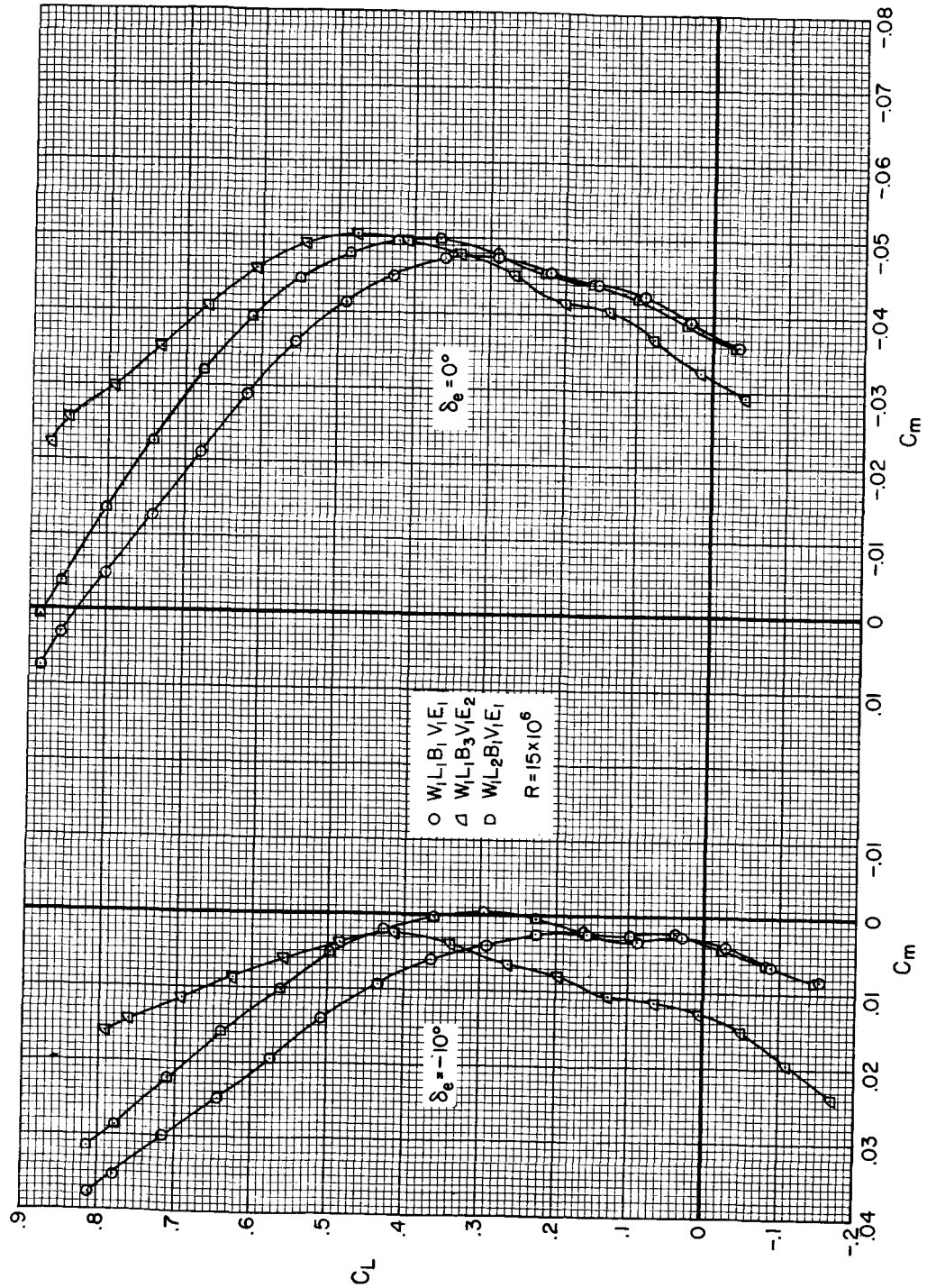

(a) C_L vs. C_m

Figure 12.- The effects of the large elevons and the modified leading edge on the longitudinal characteristics; $\beta = 0^o$, $M = 0.26$.

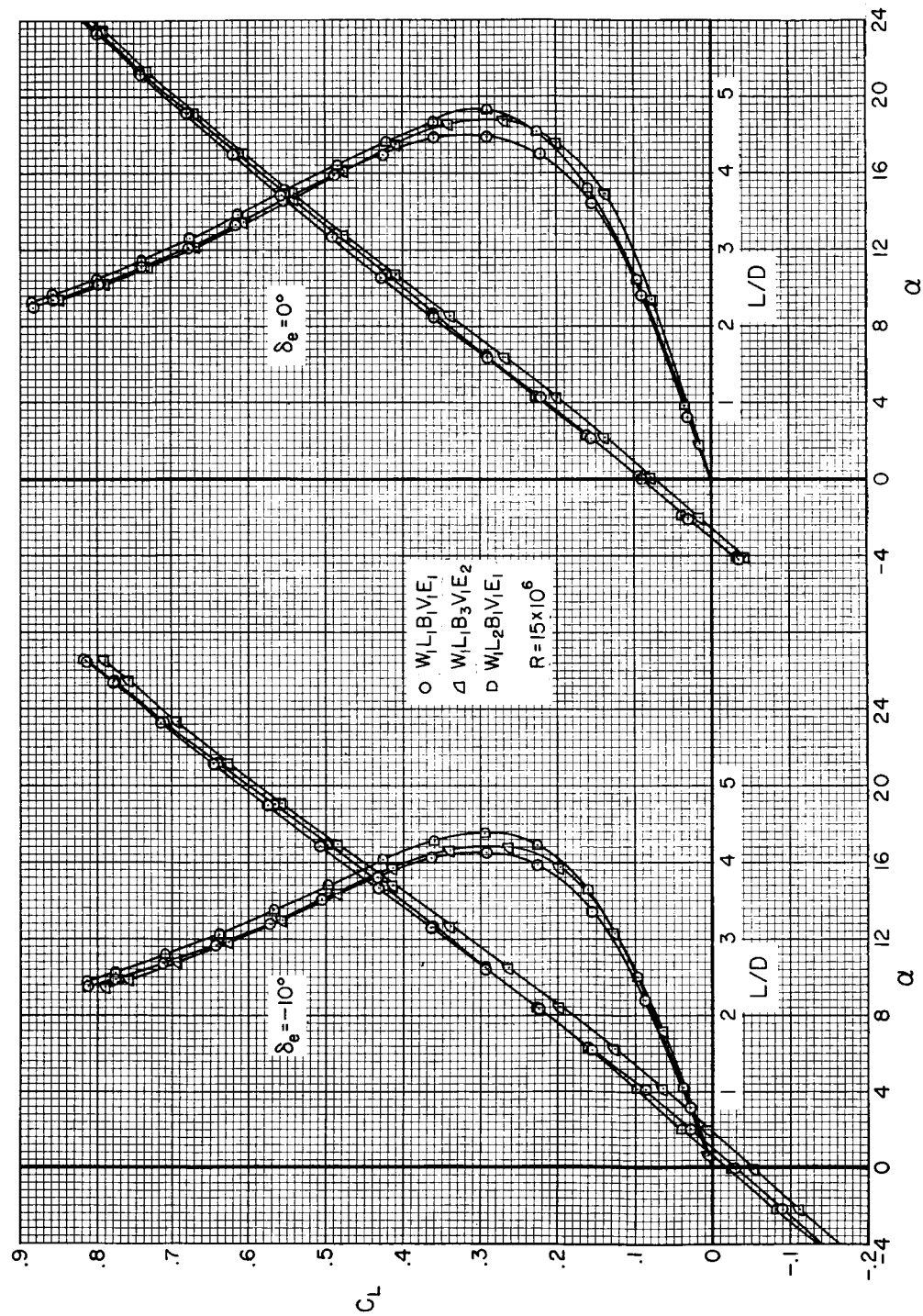

(b) C_L vs. α and C_L vs. L/D

Figure 12.- Concluded.

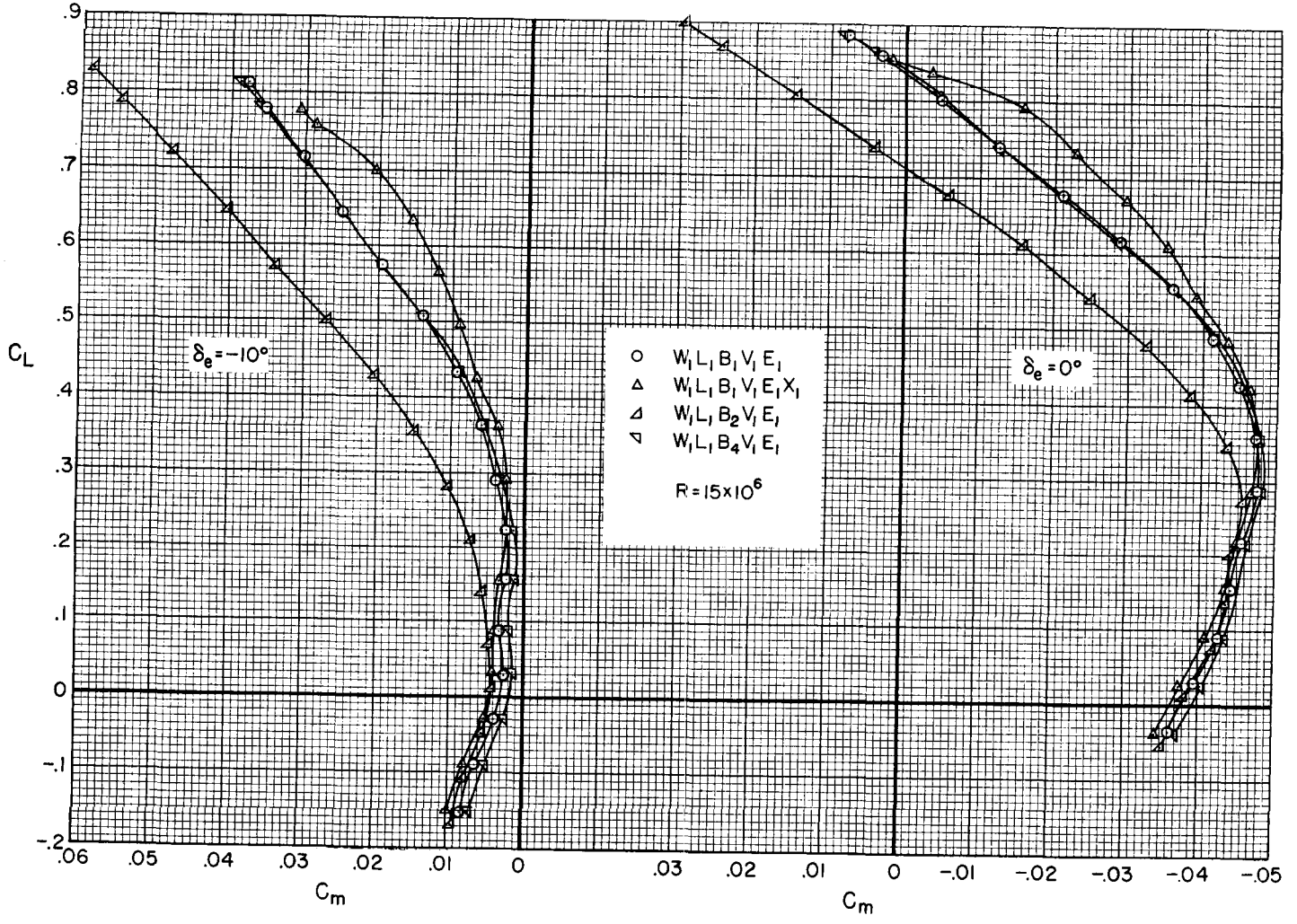

(a) C_L vs. C_m

Figure 13.- The effects of several body modifications on the longitudinal characteristics; $\beta = 0°$, $M = 0.26$.

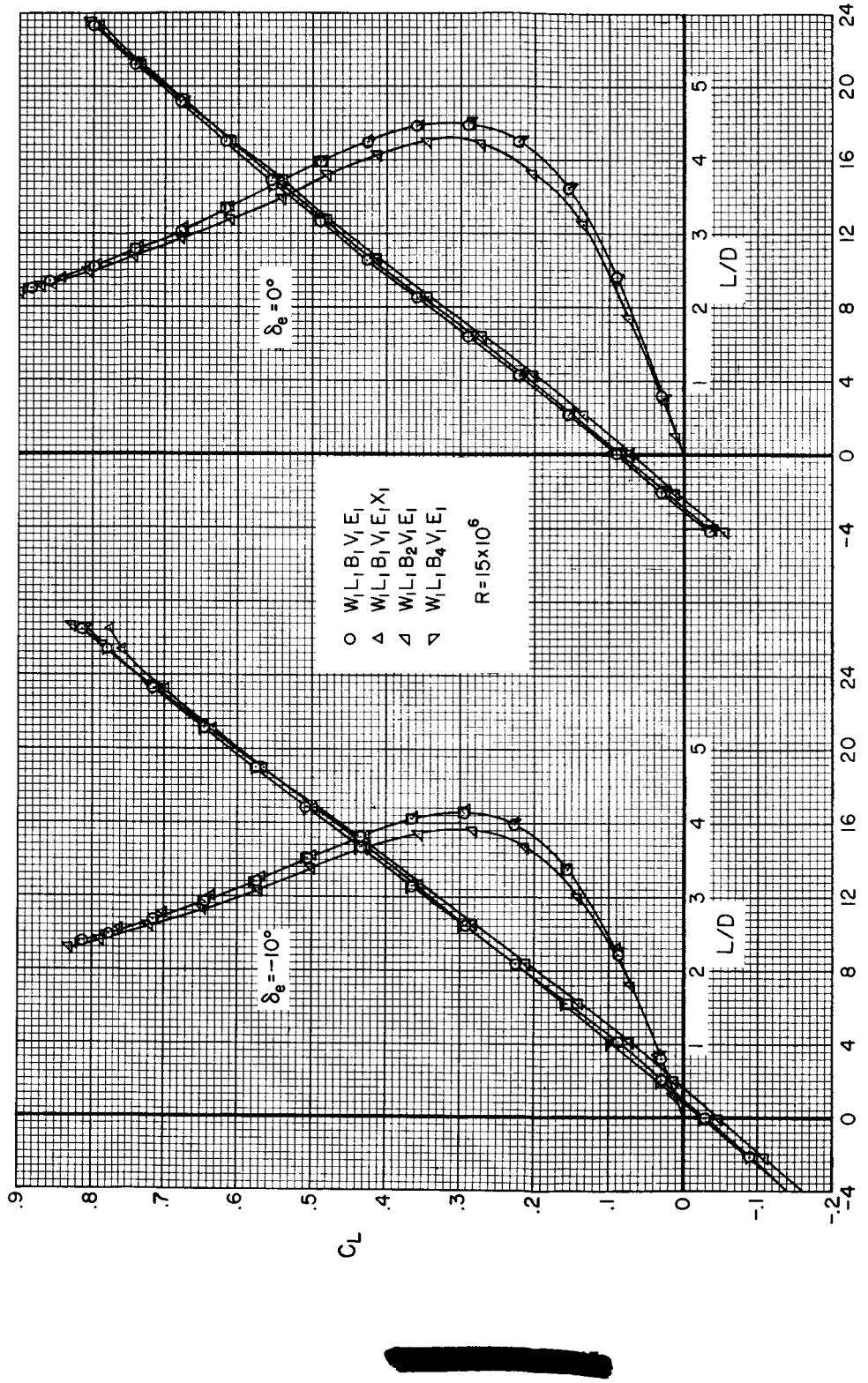

(b) C_L vs. α and C_L vs. L/D

Figure 13.- Concluded.

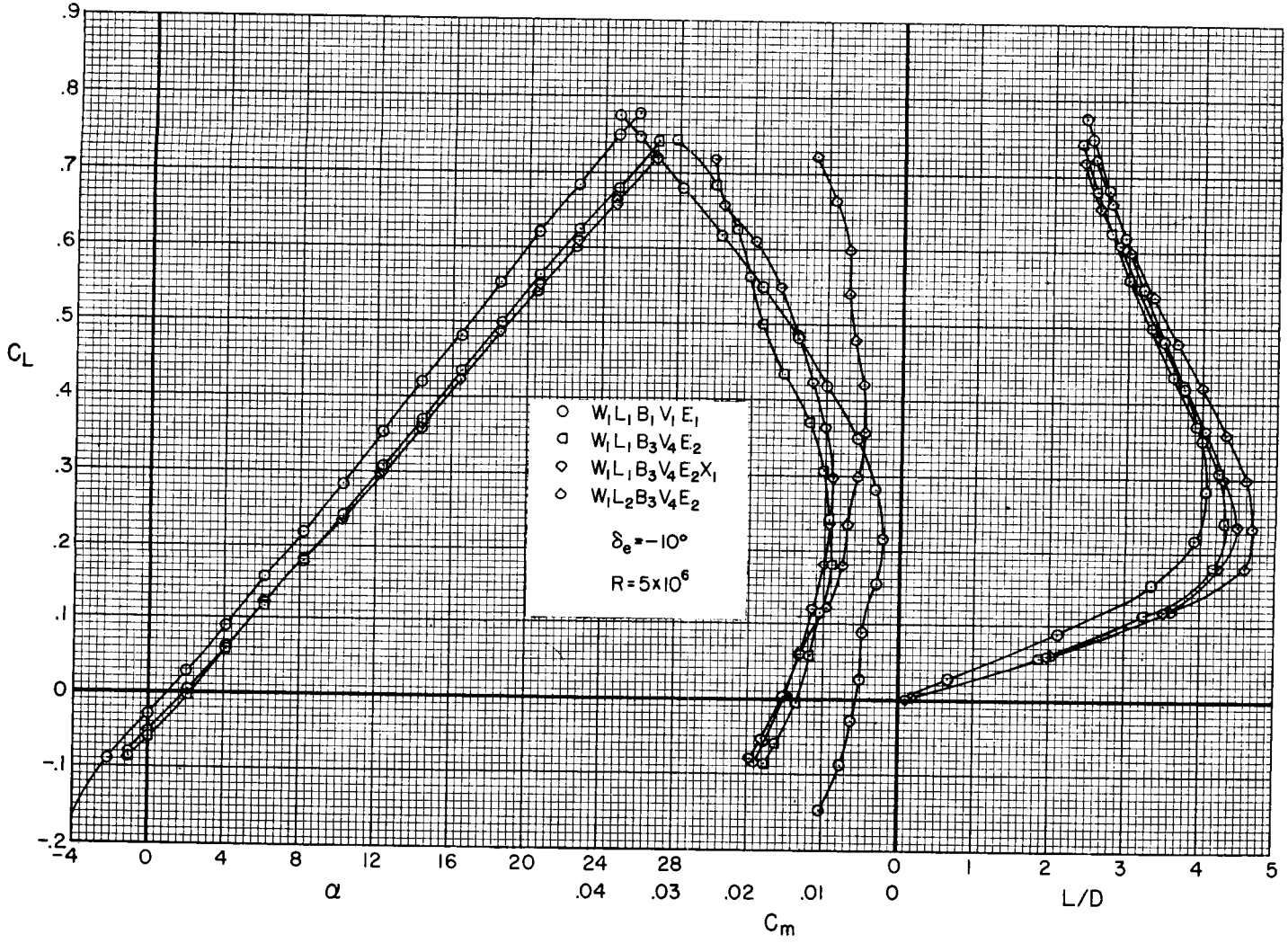

Figure 14.- The effects of the change in vertical tail toe-in with large elevons, fillets, and wing leading-edge modifications on the longitudinal characteristics; $\beta = 0°$, $M = 0.26$.

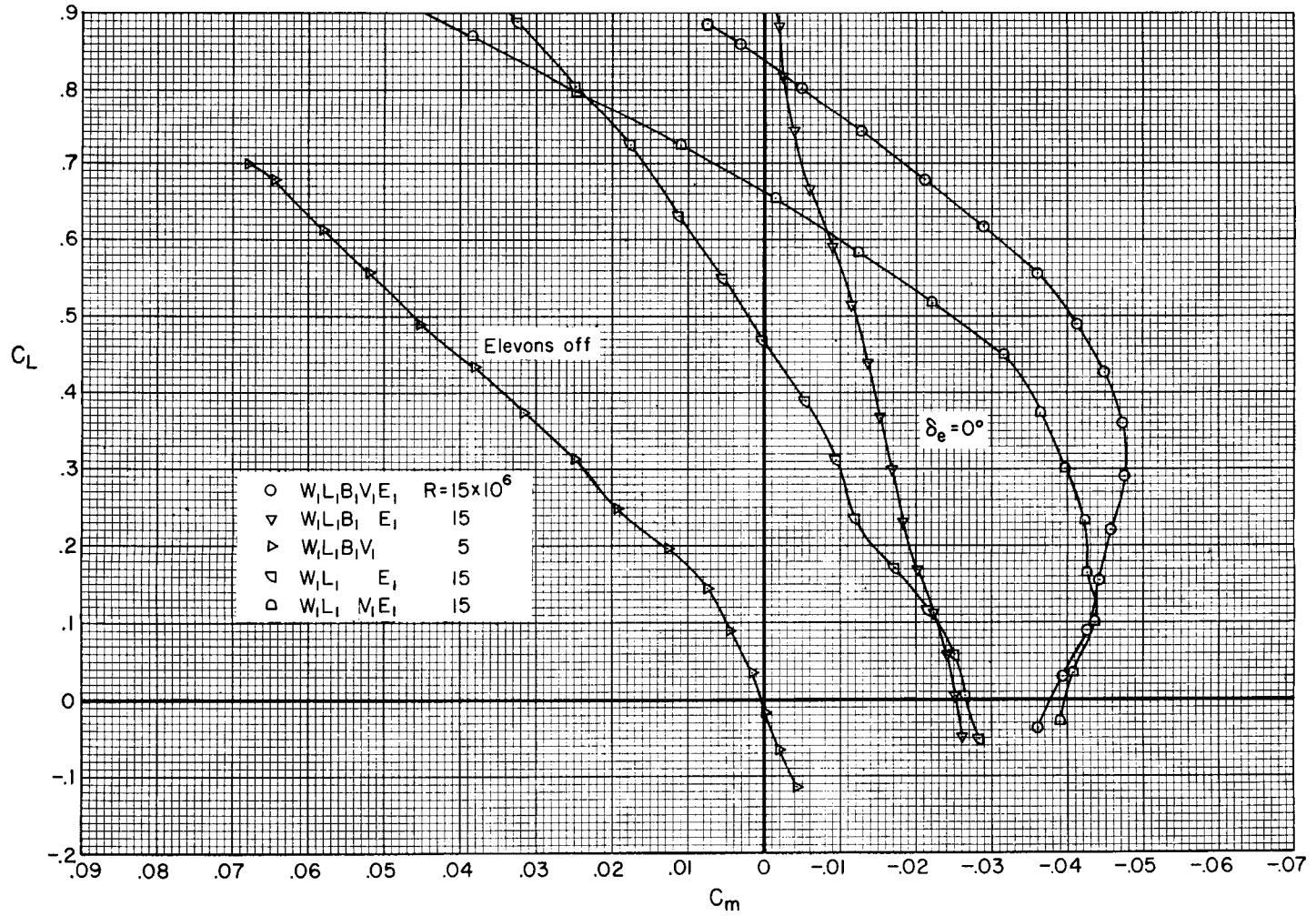

(a) C_L vs. C_m

Figure 15.- The effects of removing various components on the longitudinal characteristics; $\beta = 0^o$, $M = 0.26$.

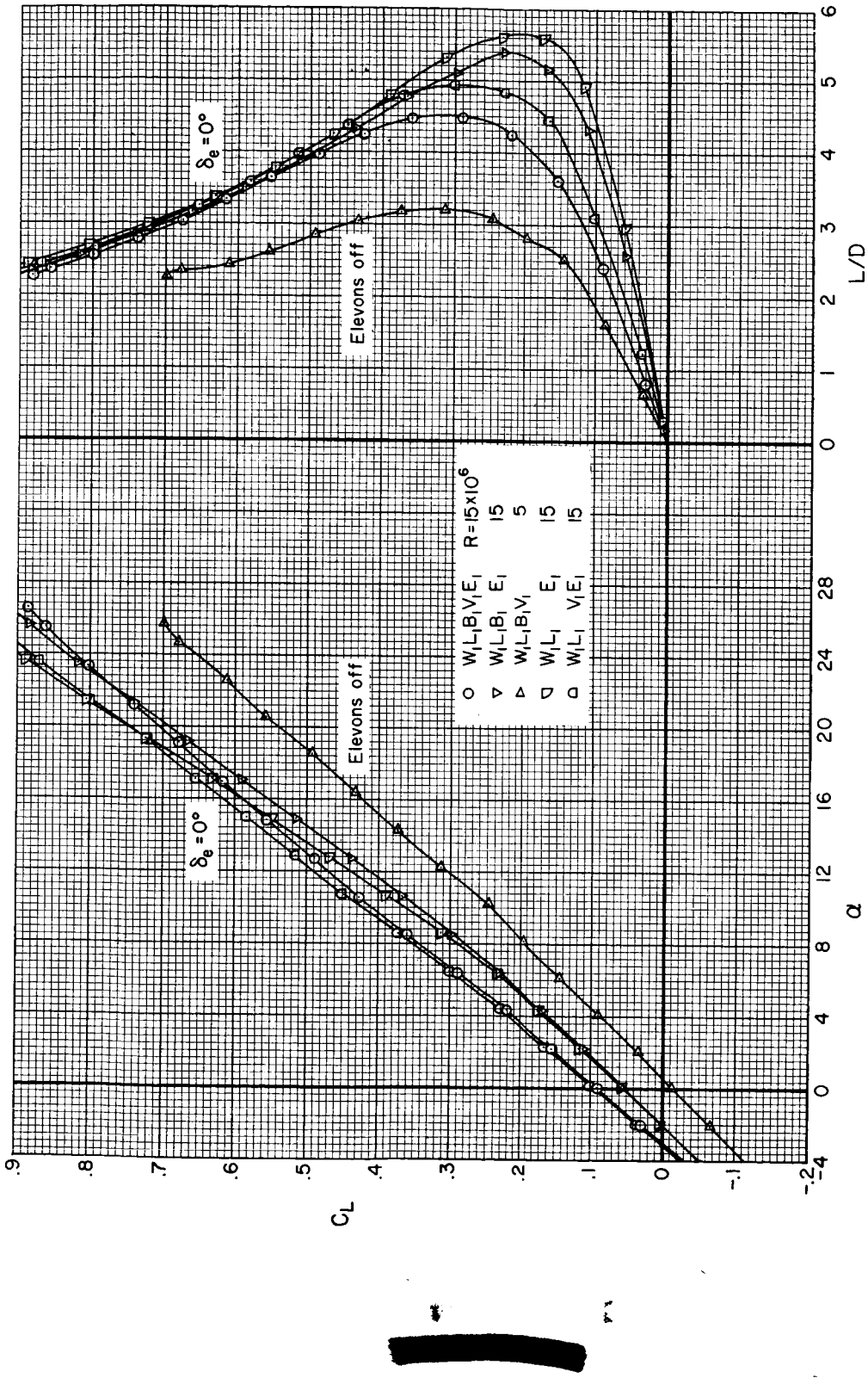

(b) C_L vs. α and C_L vs. L/D

Figure 15.- Concluded.

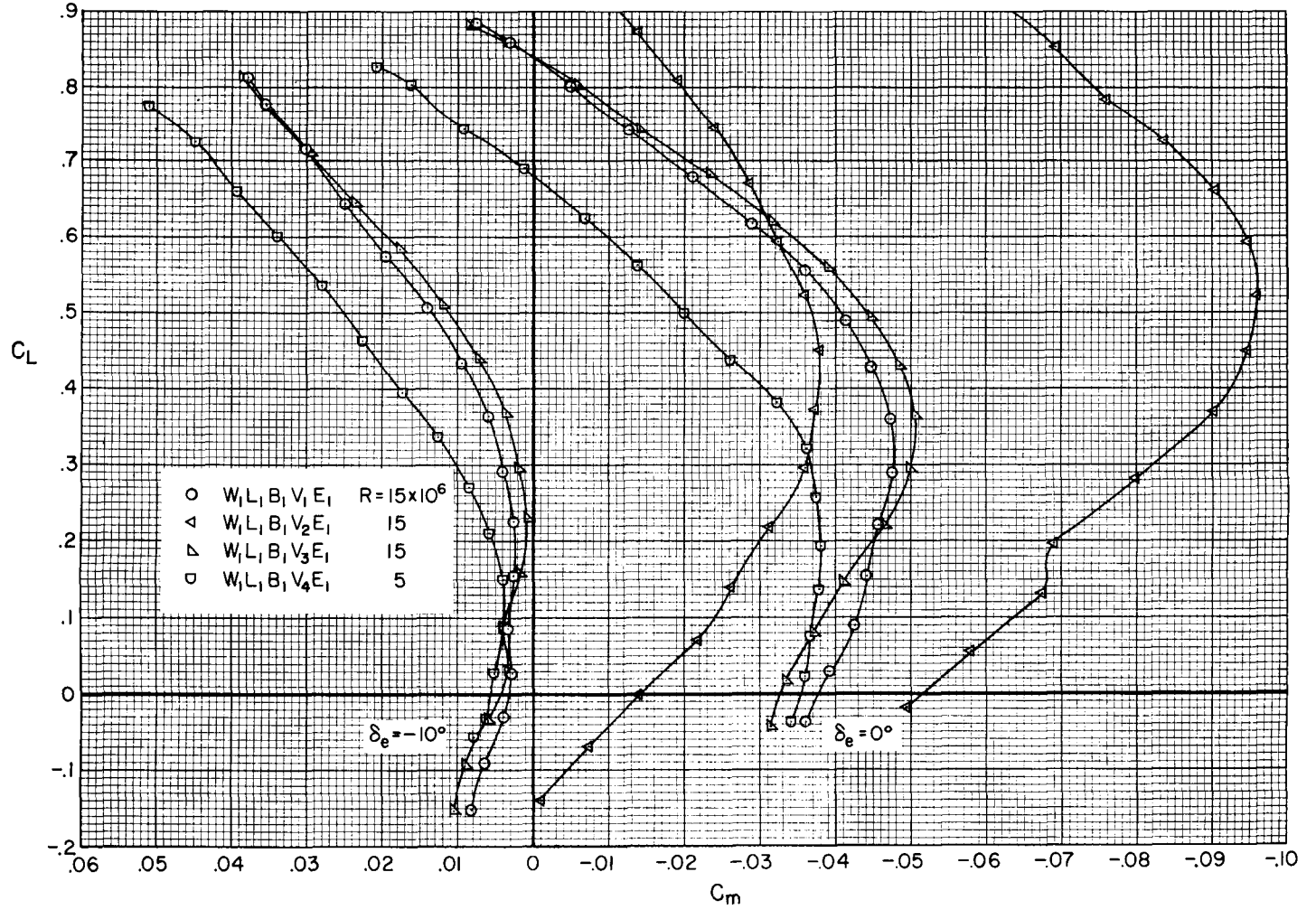

(a) C_L vs. C_m

Figure 16.- The effects of vertical tail modifications on the longitudinal characteristics; $\beta = 0^\circ$, $M = 0.26$.

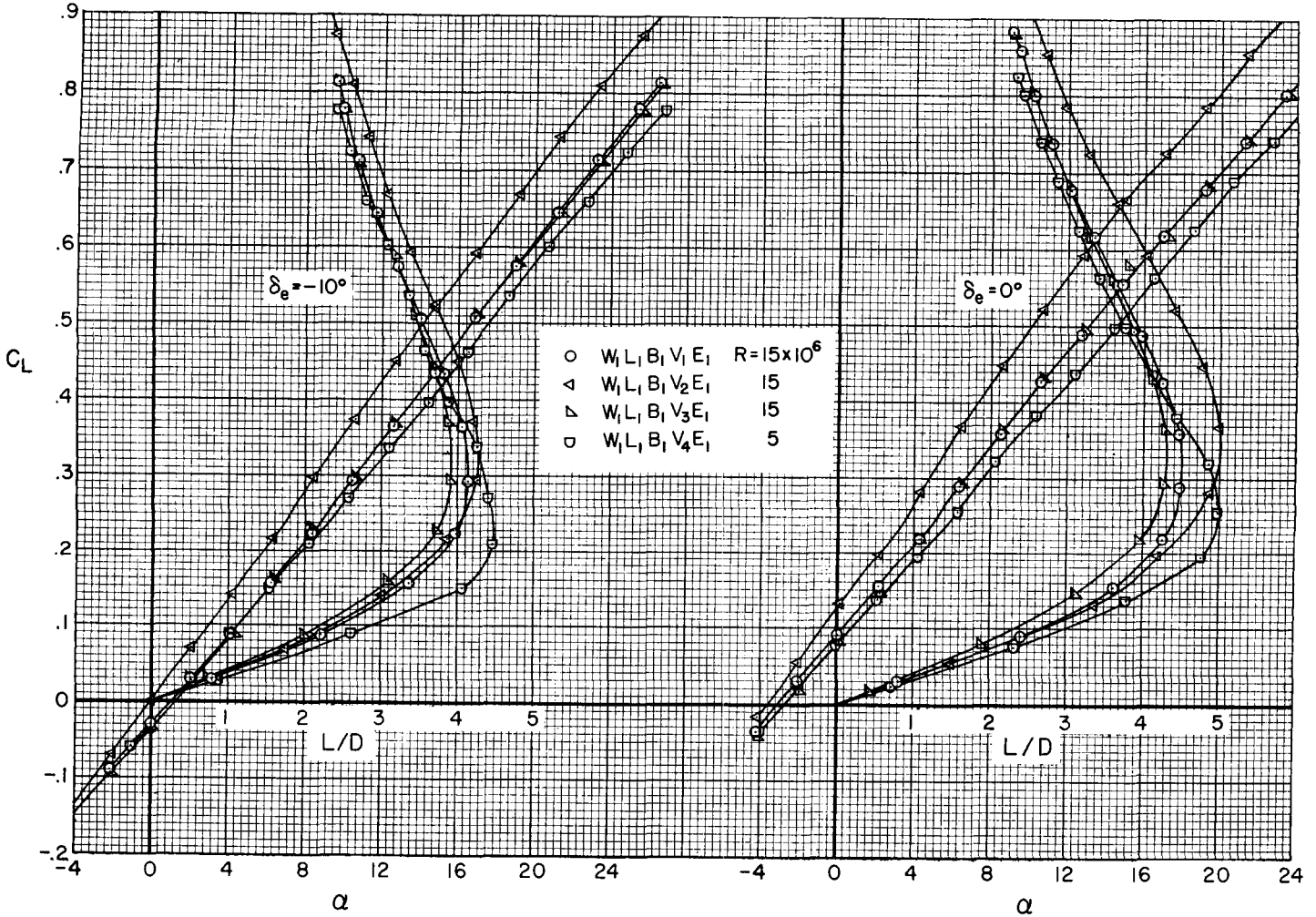

(b) C_L vs. α and C_L vs. L/D

Figure 16.- Concluded.

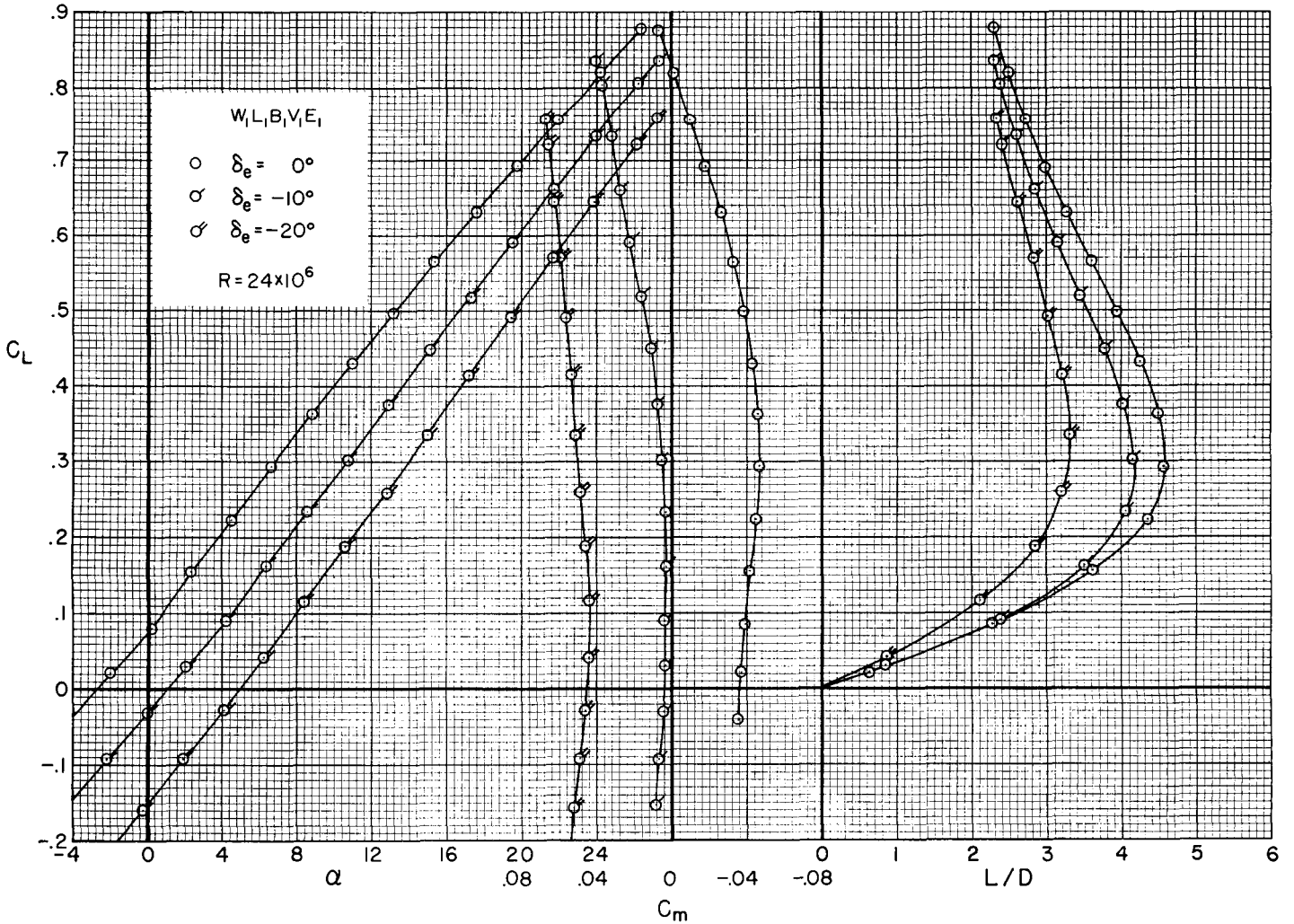

Figure 17.- The longitudinal characteristics for several elevon deflections; $\beta = 0^{o}$, M = 0.26.

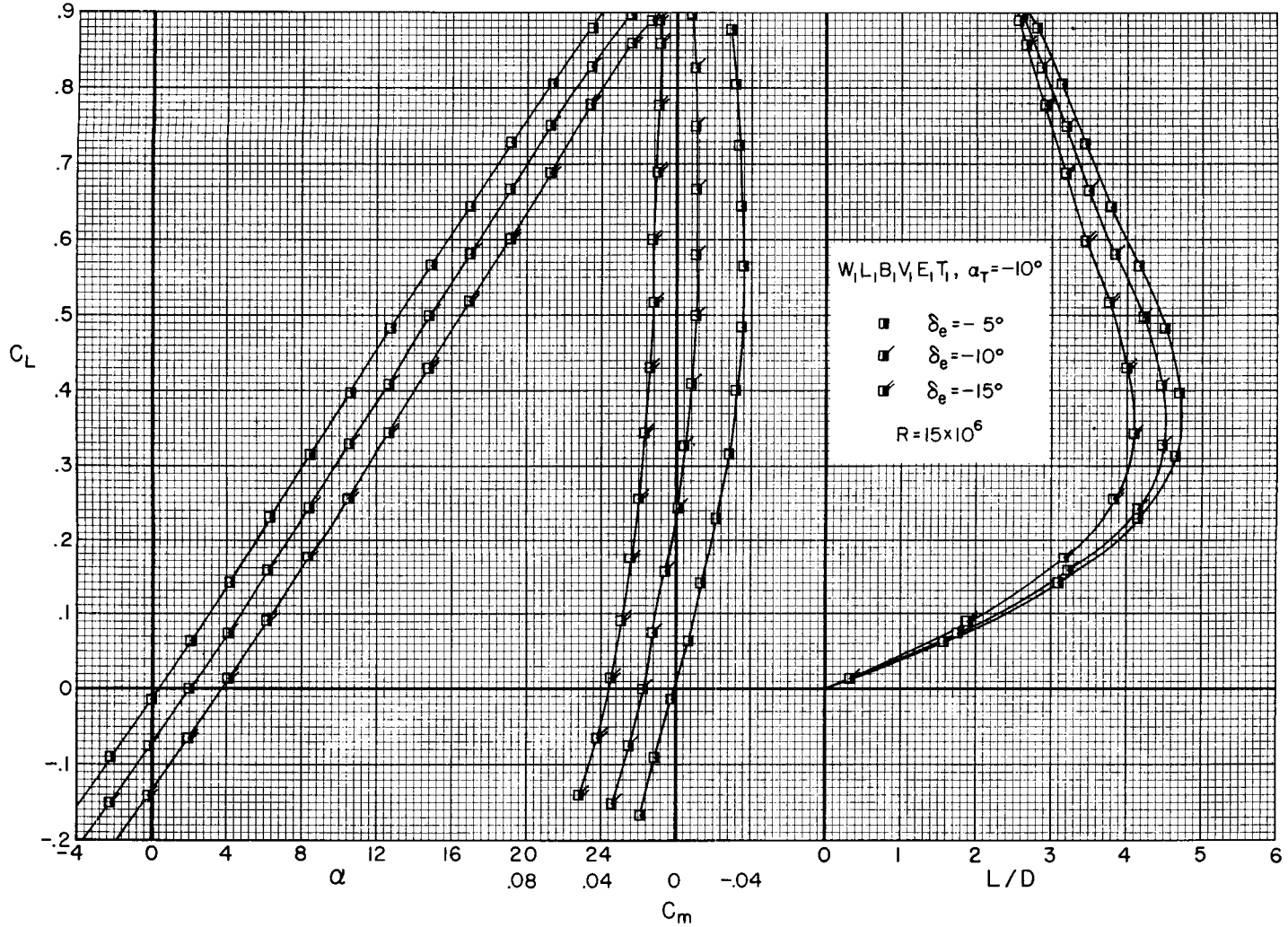

Figure 18.- The longitudinal characteristics of the model with large wing-tip extensions and several elevon deflections; $\beta = 0^o$, $M = 0.26$.

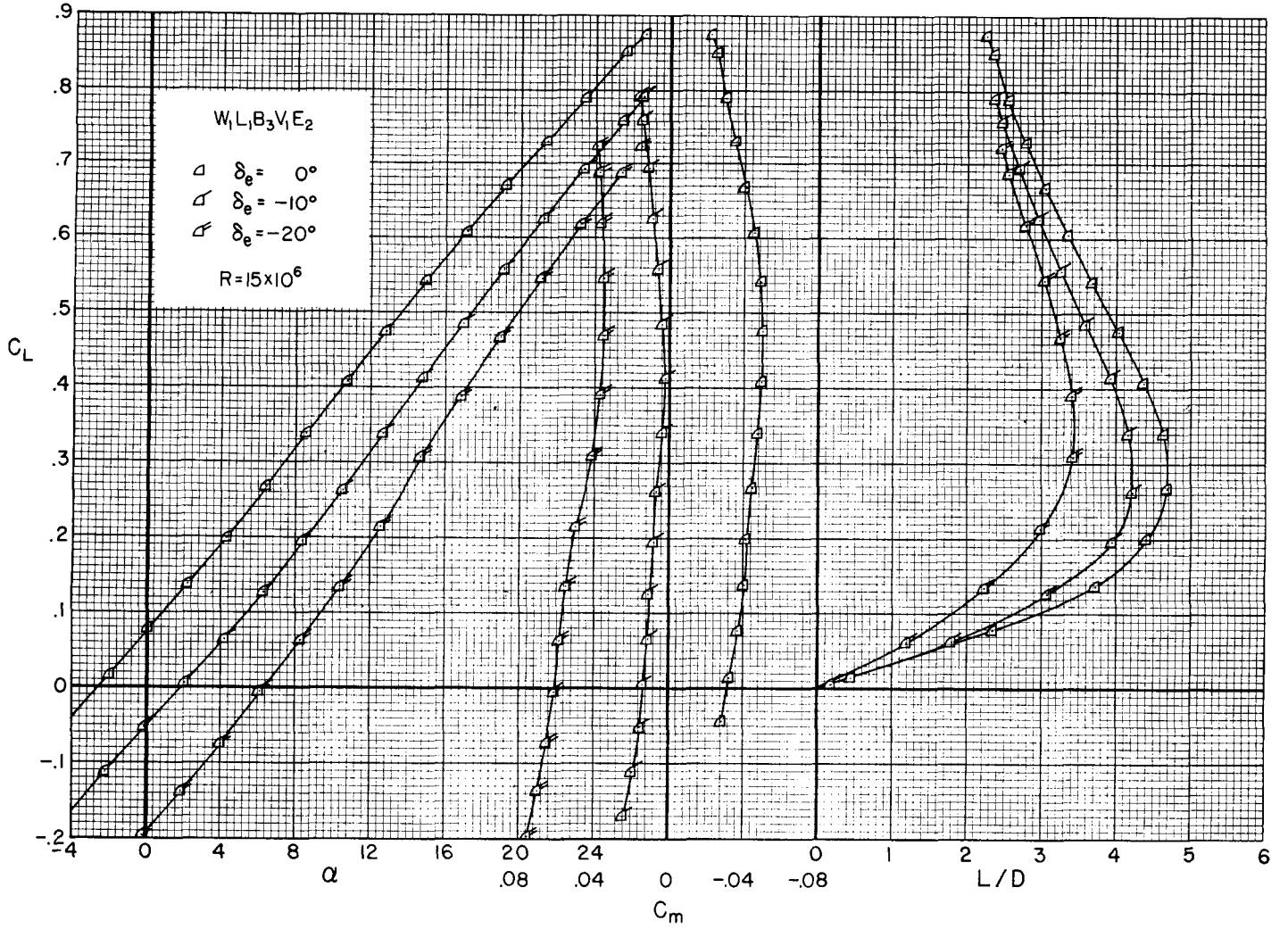

Figure 19.- The longitudinal characteristics of the model with large elevons at several elevon ddeflections; $\beta = 0^{o}$, $M = 0.26$.

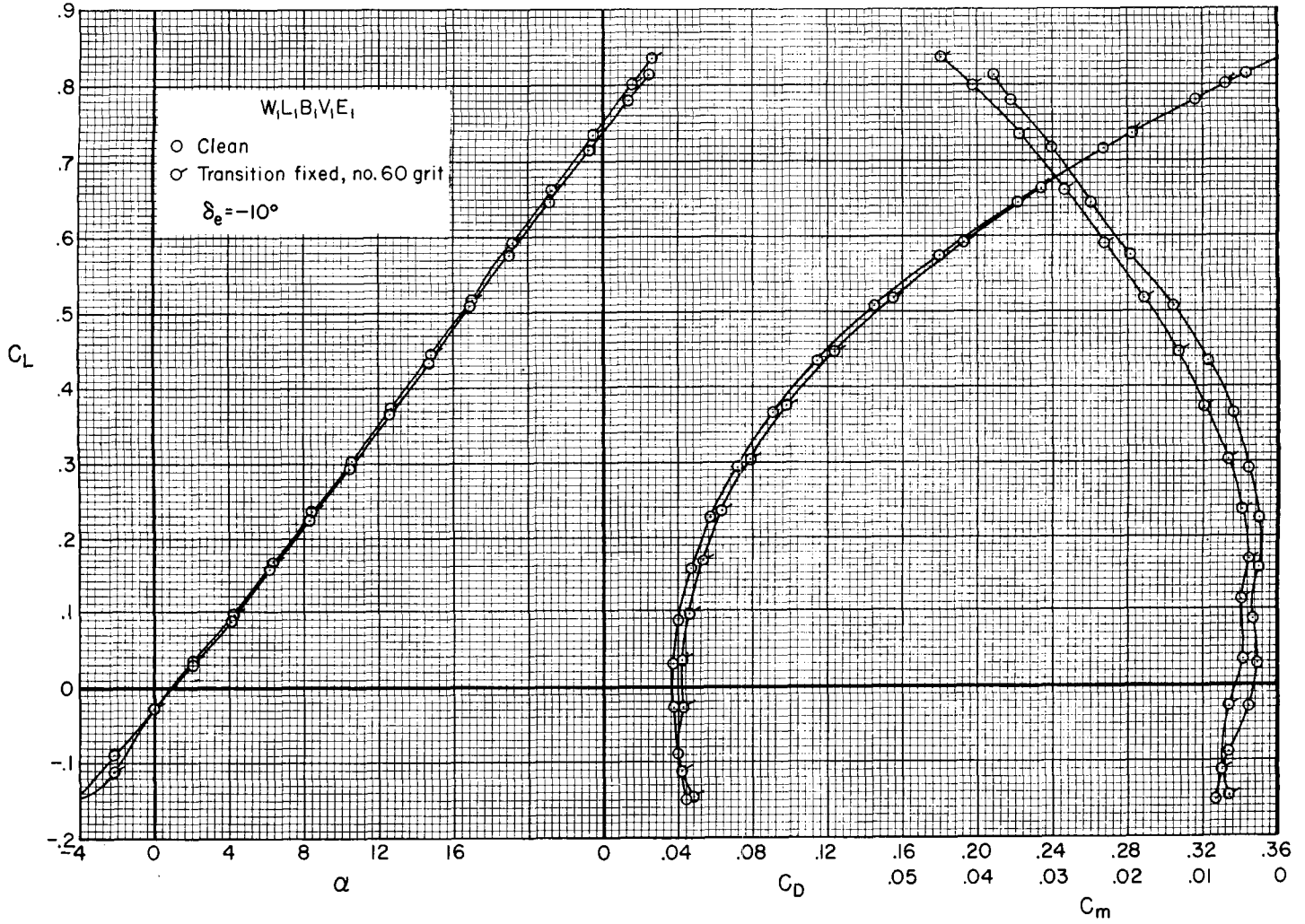

(a) $R = 15 \times 10^6$

Figure 20.- The effects of leading-edge transition strips on the longitudinal characteristics; $\beta = 0°$, $M = 0.26$.

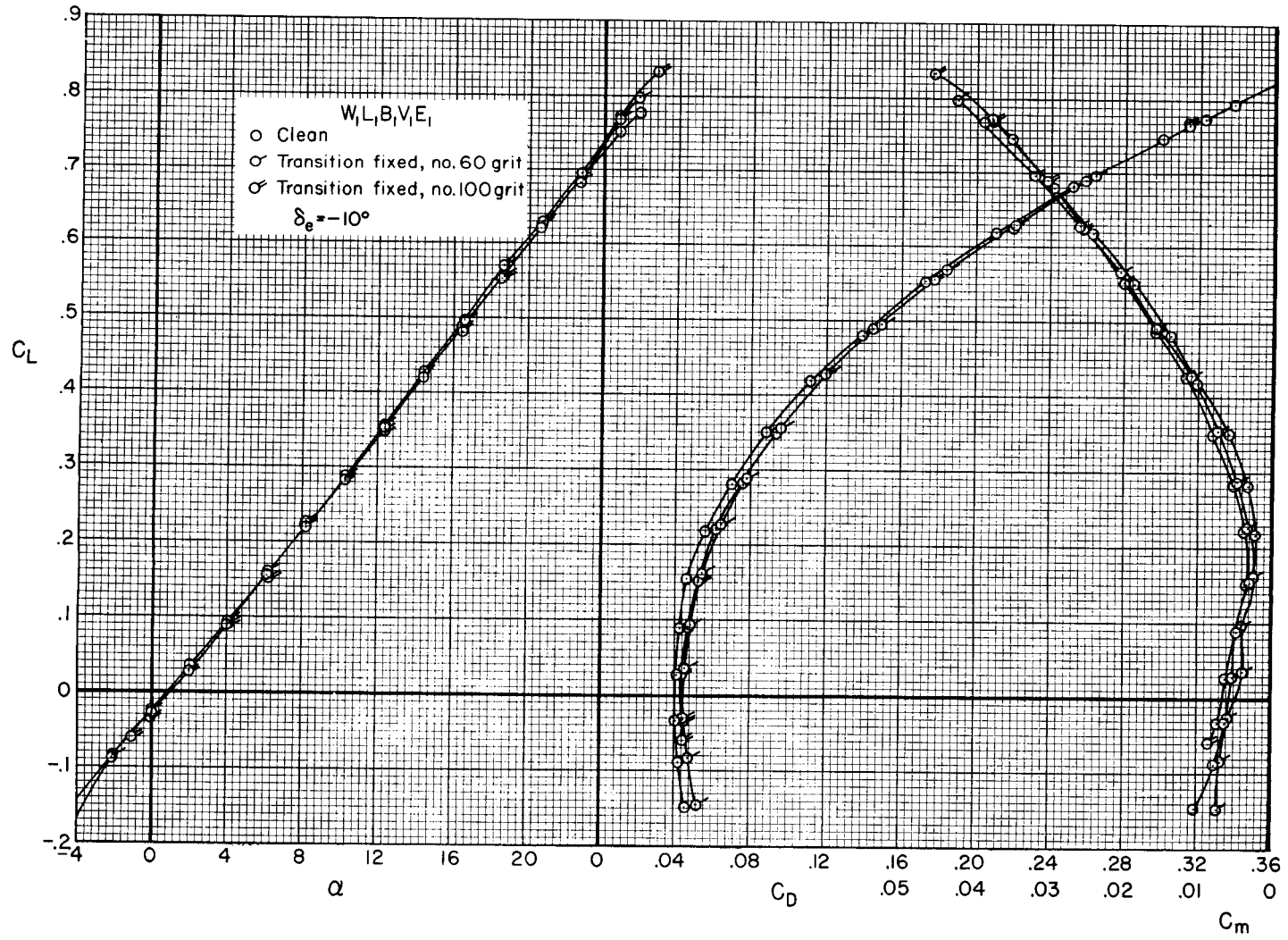

(b) R = 5×10^6

Figure 20.- Concluded.

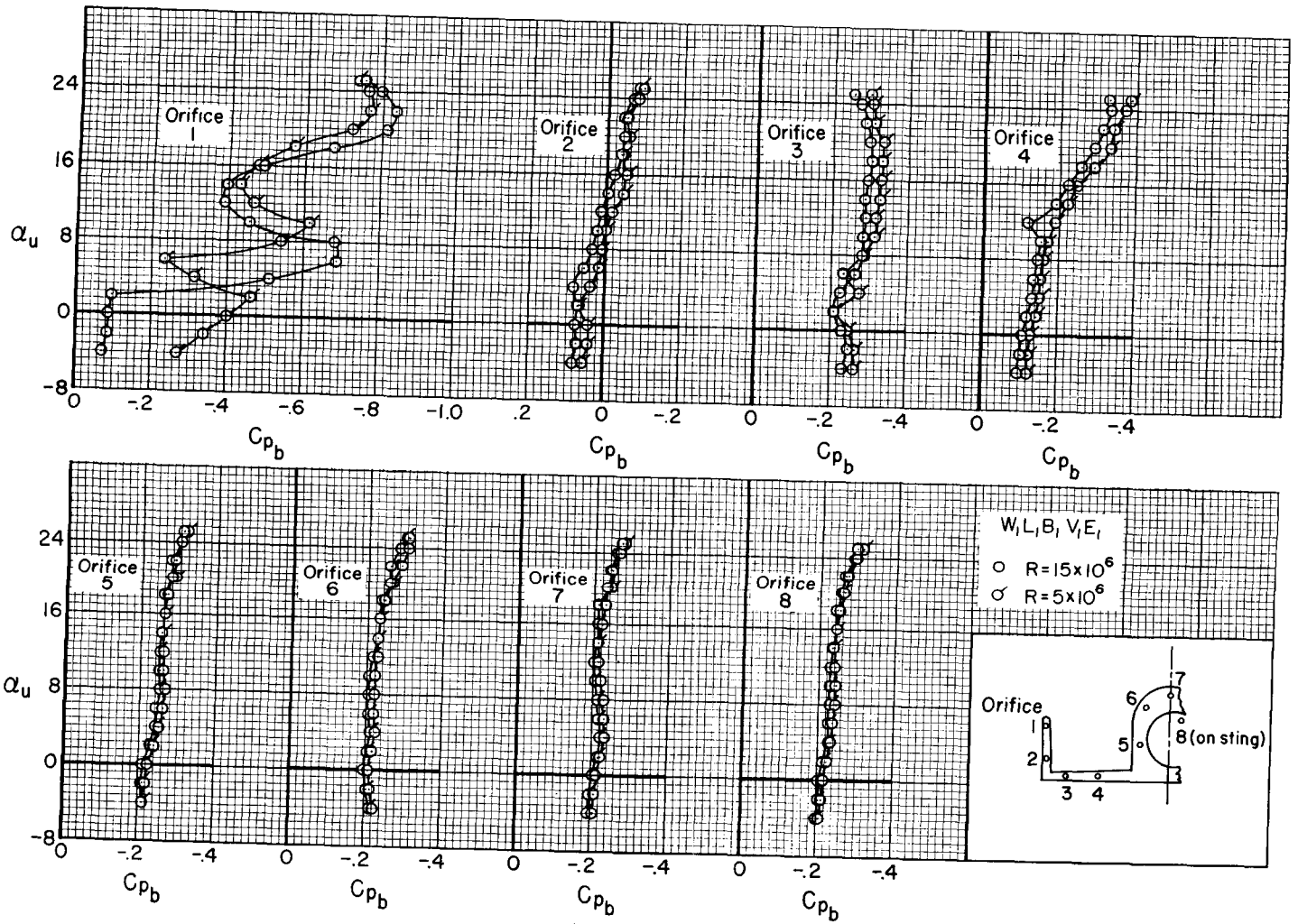

Figure 21.- Model base pressures; $\delta_e = 0^o$, $\beta = 0^o$, M = 0.26.

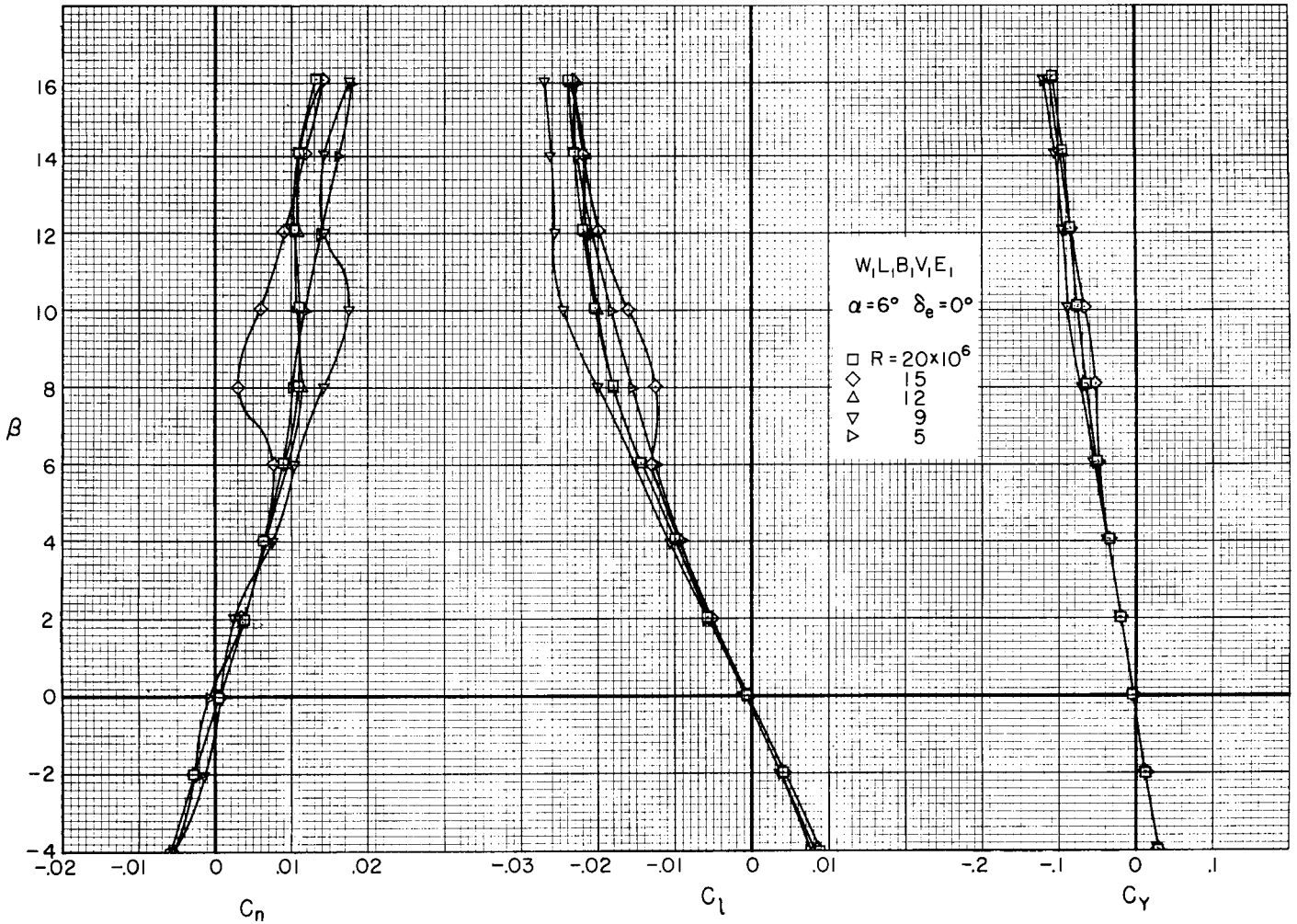

(a) Standard model.

Figure 22.- The effects of Reynolds number on the lateral-directional characteristics as functions of angle of sideslip; M = 0.26.

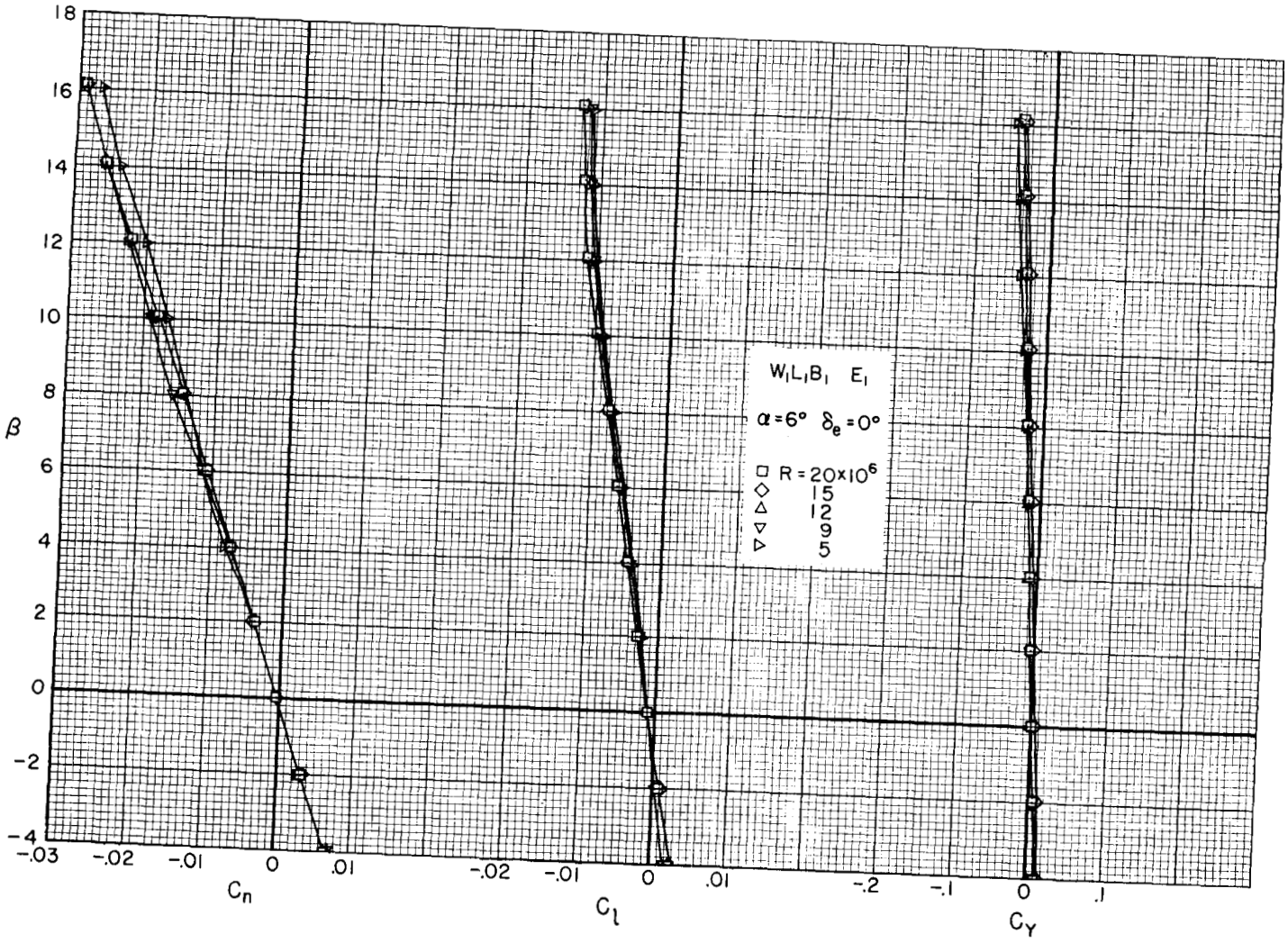

(b) Vertical tails off.

Figure 22.- Continued.

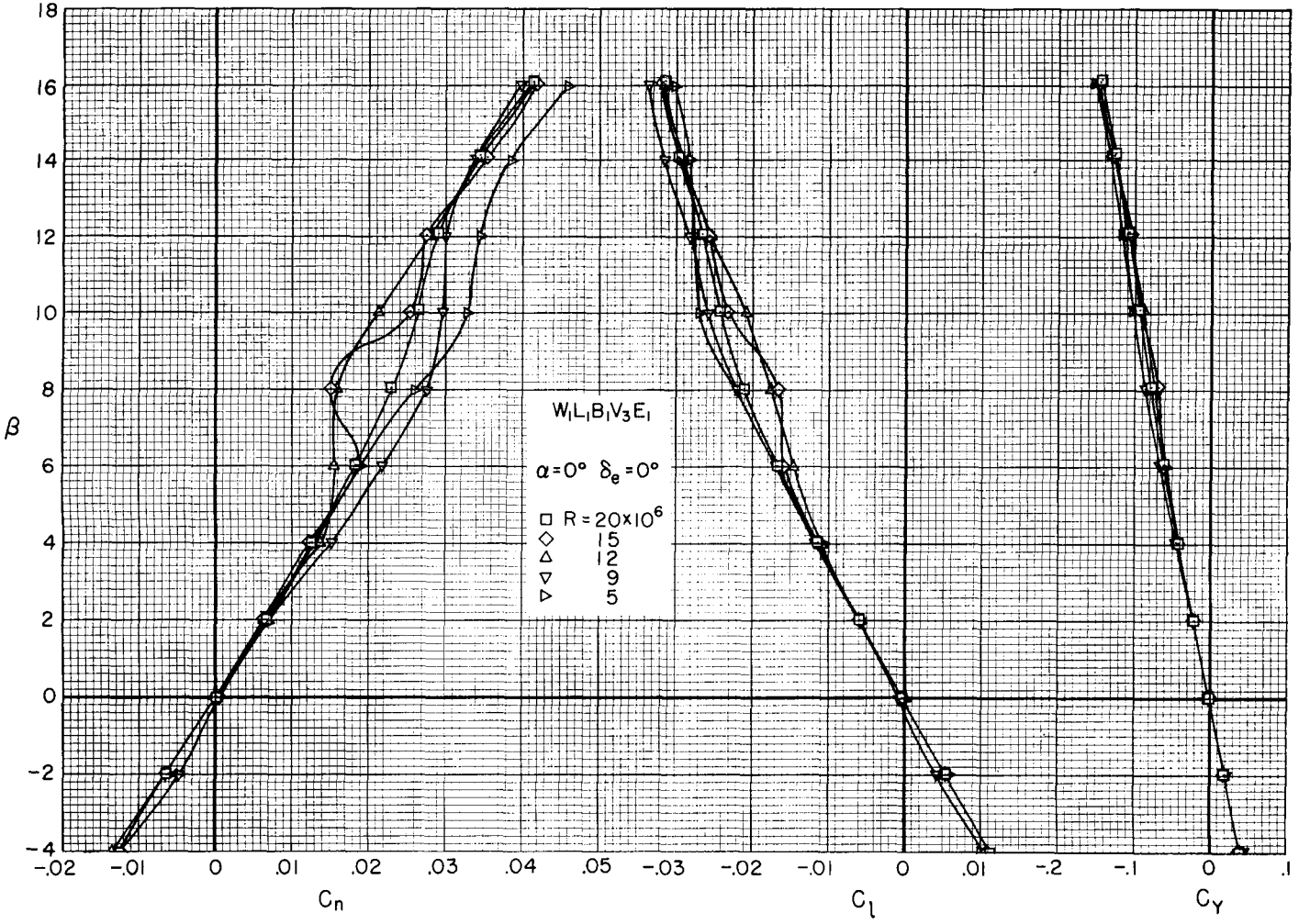

(c) Large vertical tails.

Figure 22.- Continued.

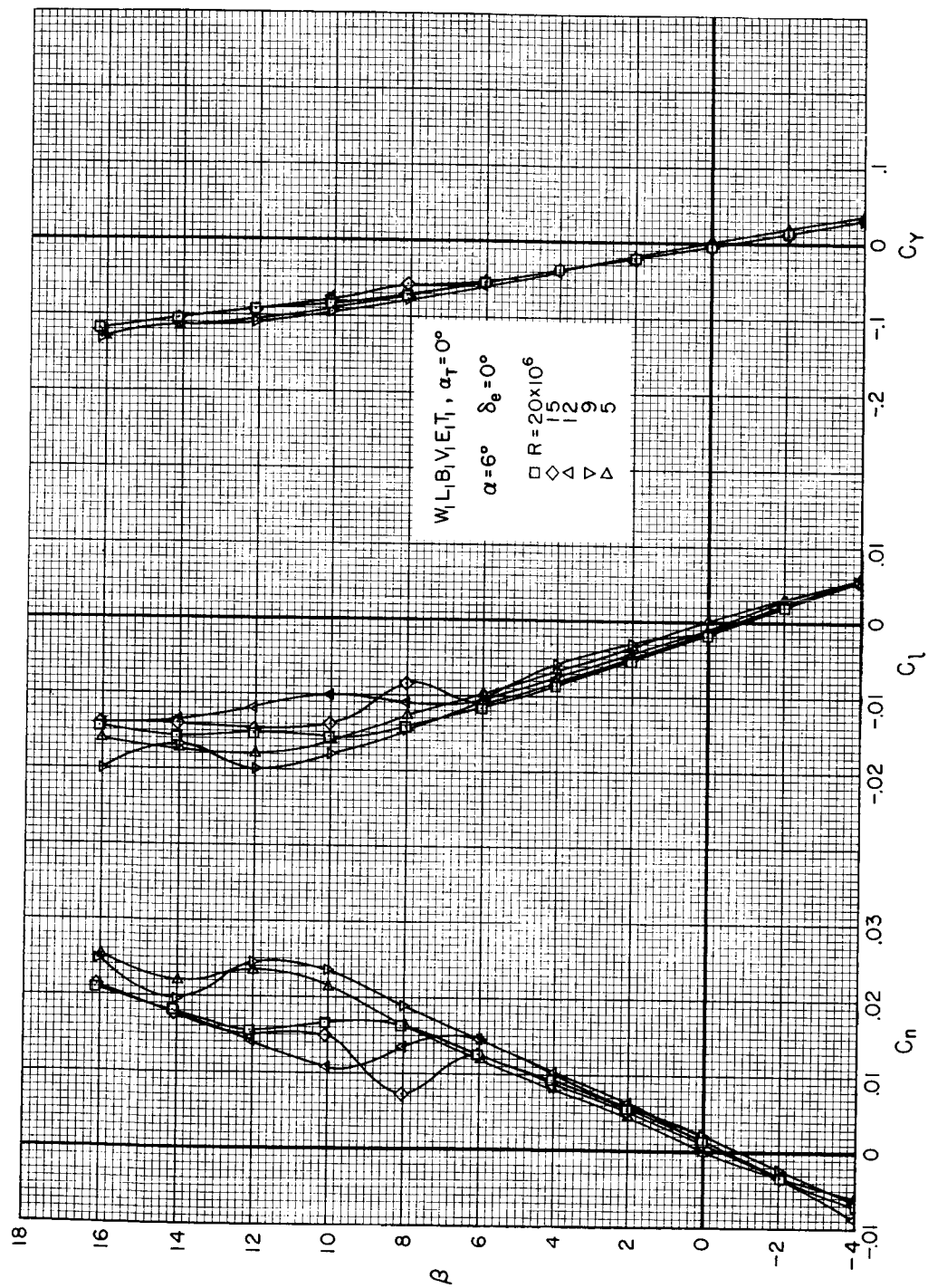

(d) Wing-tip extensions.

Figure 22.- Continued.

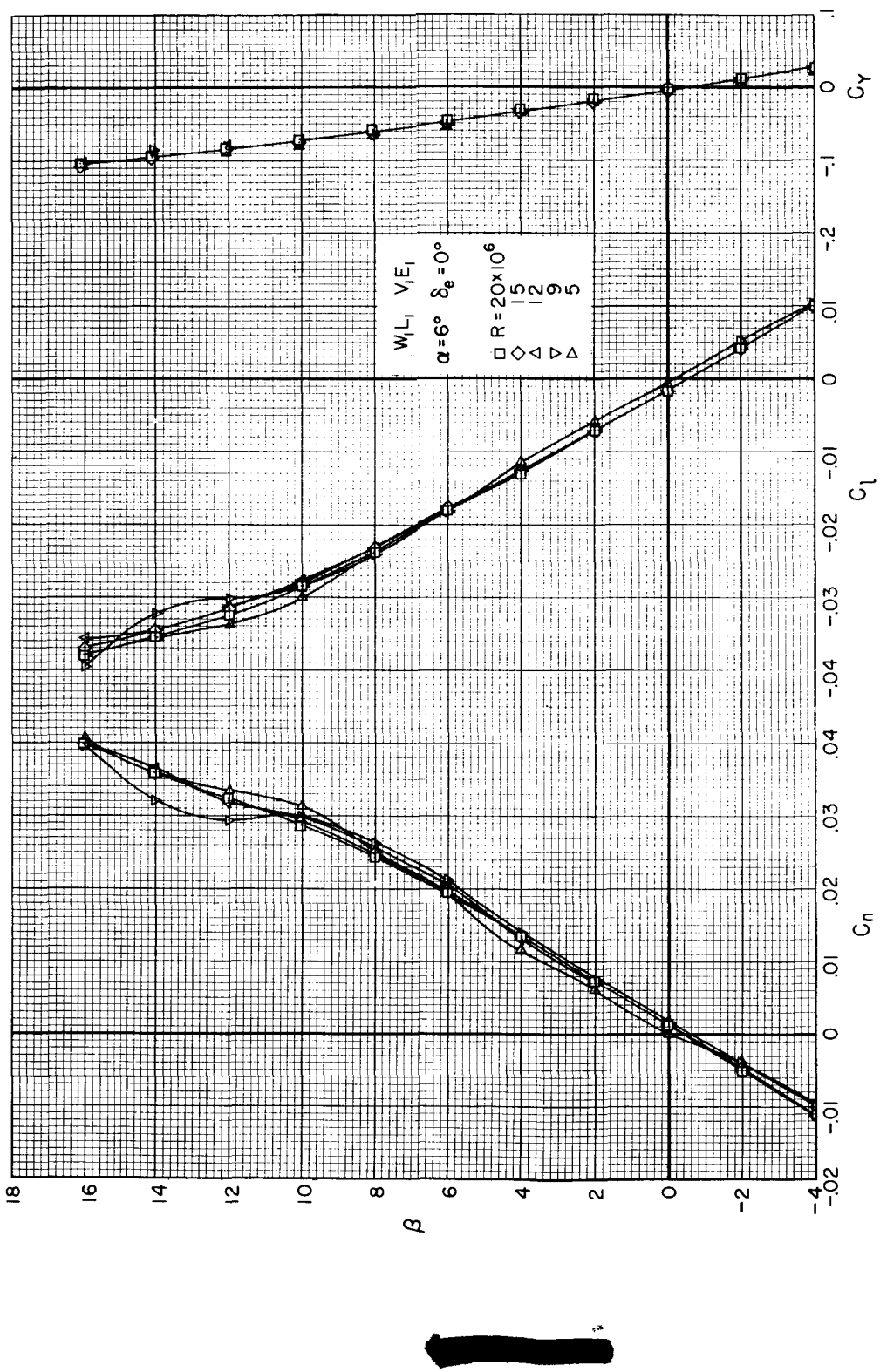

(e) Body removed.

Figure 22.- Concluded.

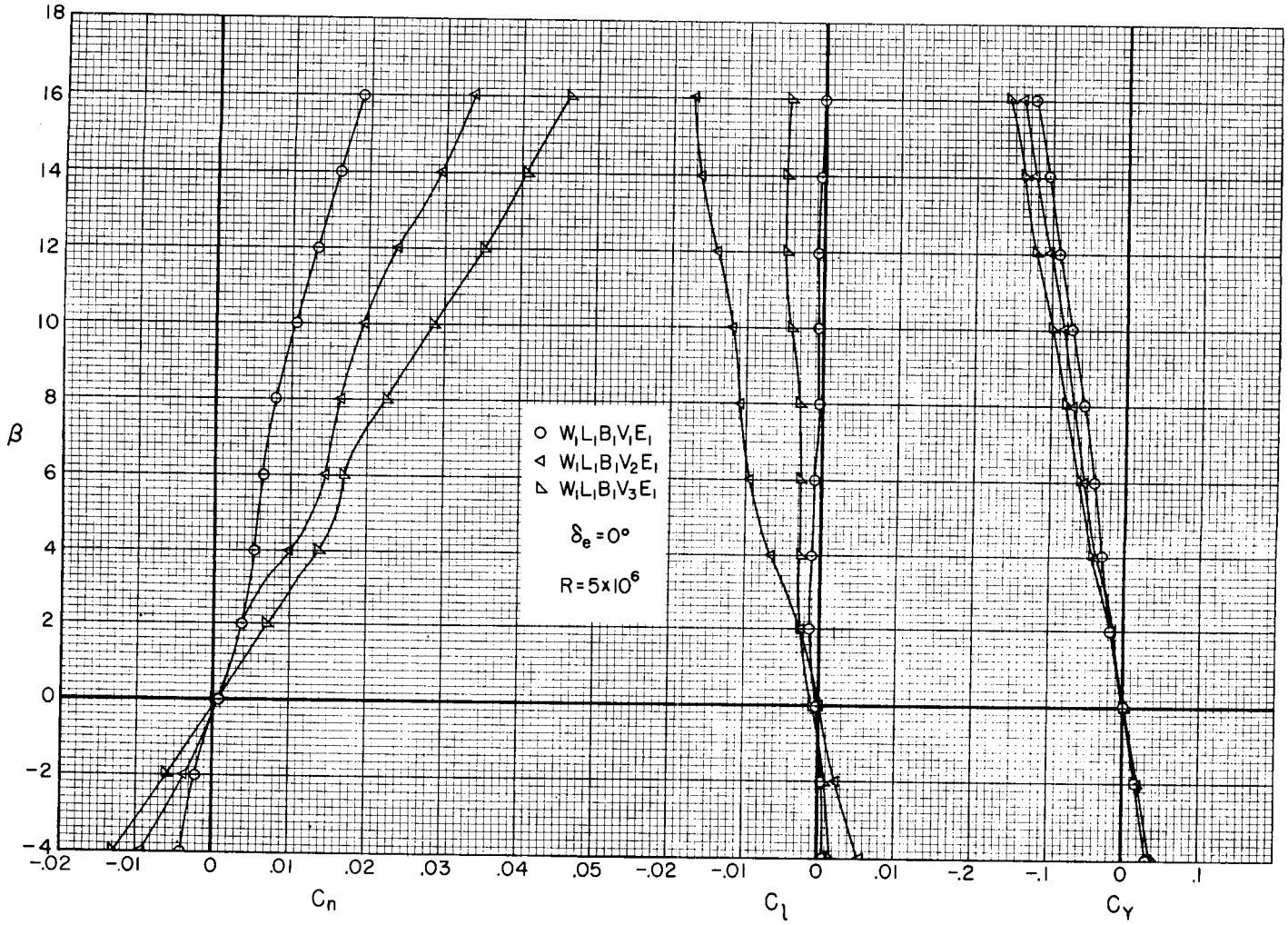

(a) $\alpha = 0^\circ$

Figure 23.- The effects of vertical tail modifications on the lateral-directional characteristics as functions of angle of sideslip; M = 0.26.

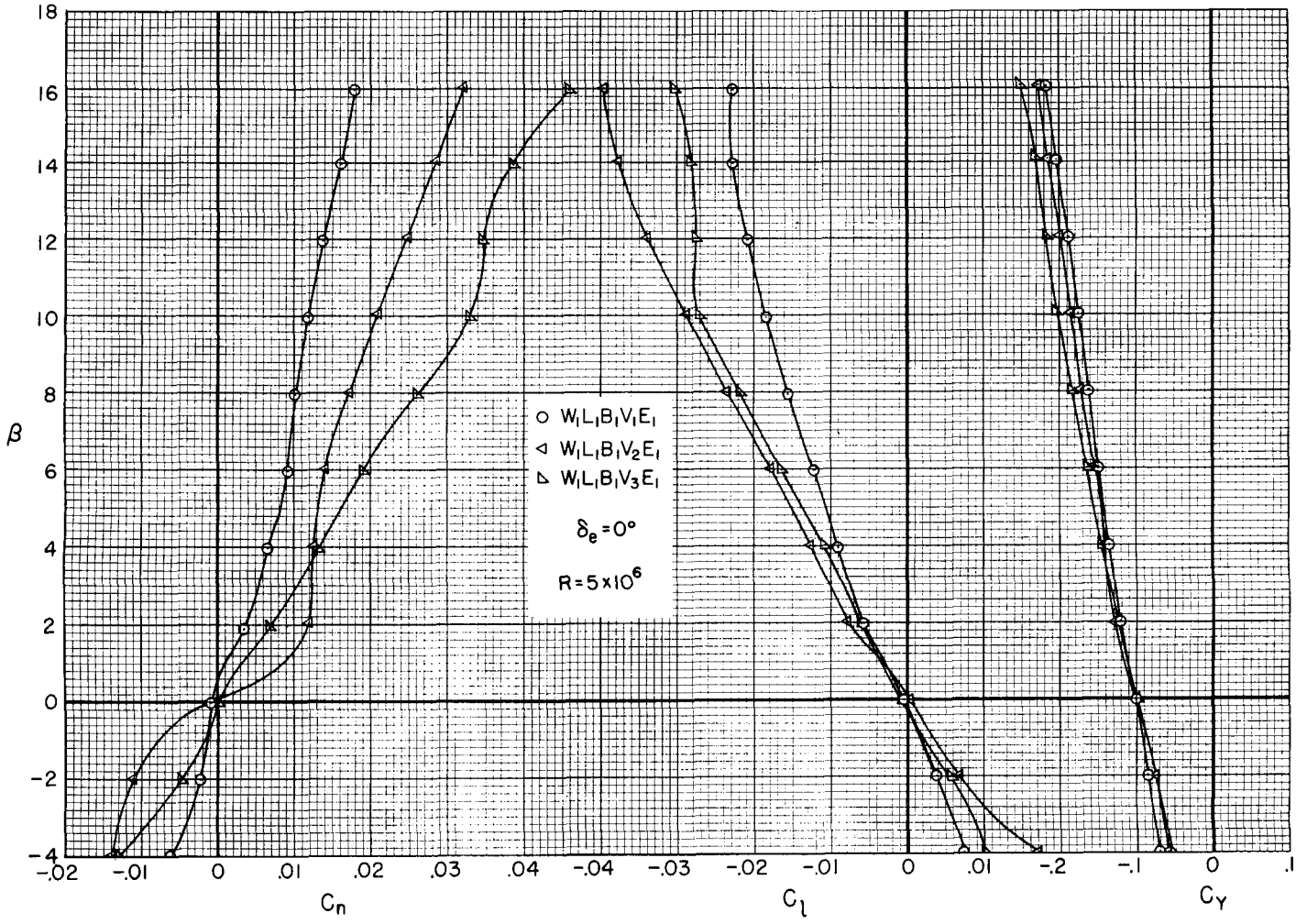

(b) $\alpha = 6^\circ$

Figure 23.- Concluded.

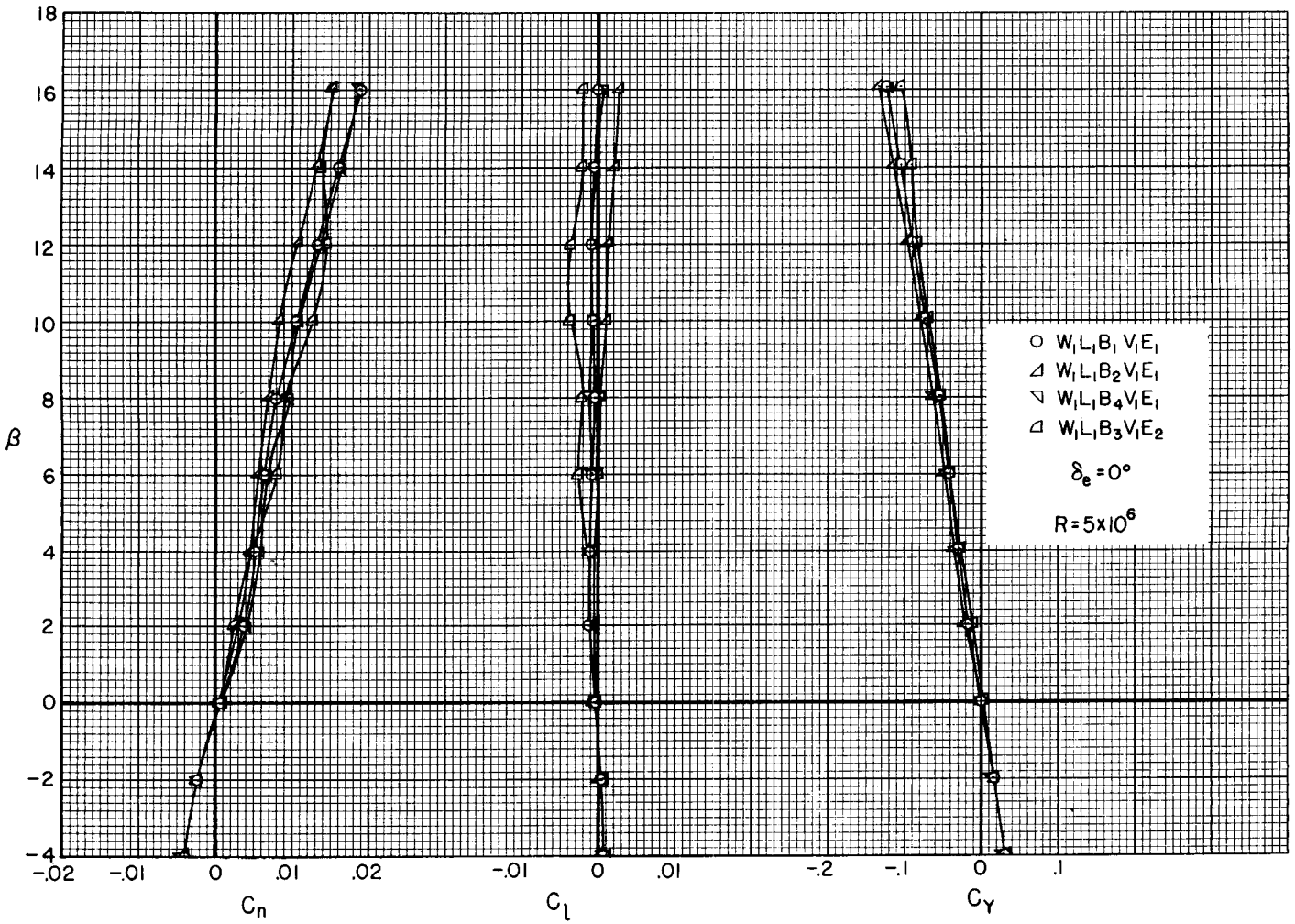

(a) $\alpha = 0^\circ$

Figure 24.- The effects of body modifications and the large elevons on the lateral-directional characteristics as functions of angle of sideslip; M = 0.26.

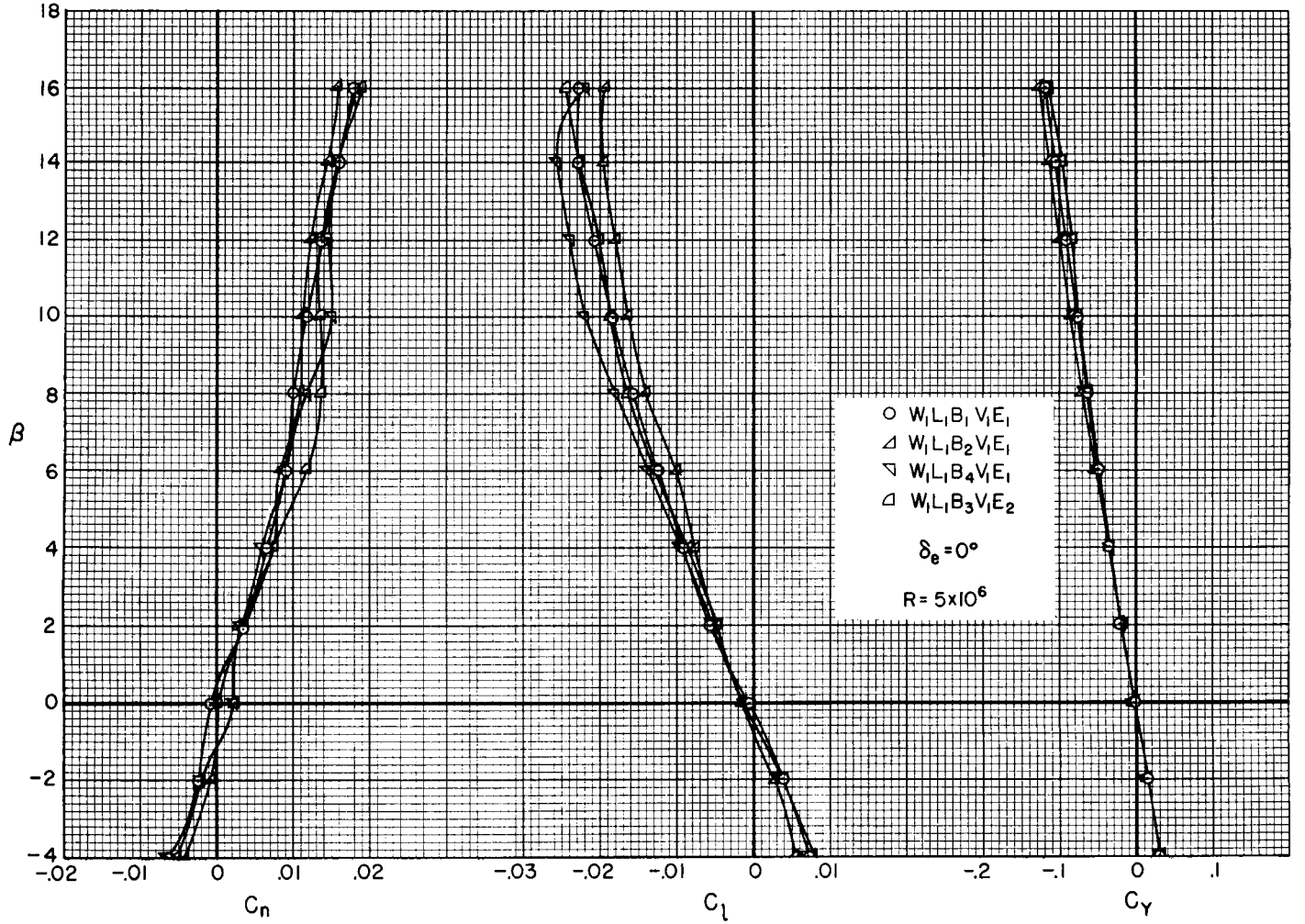

(b) $\alpha = 6°$

Figure 24.- Continued.

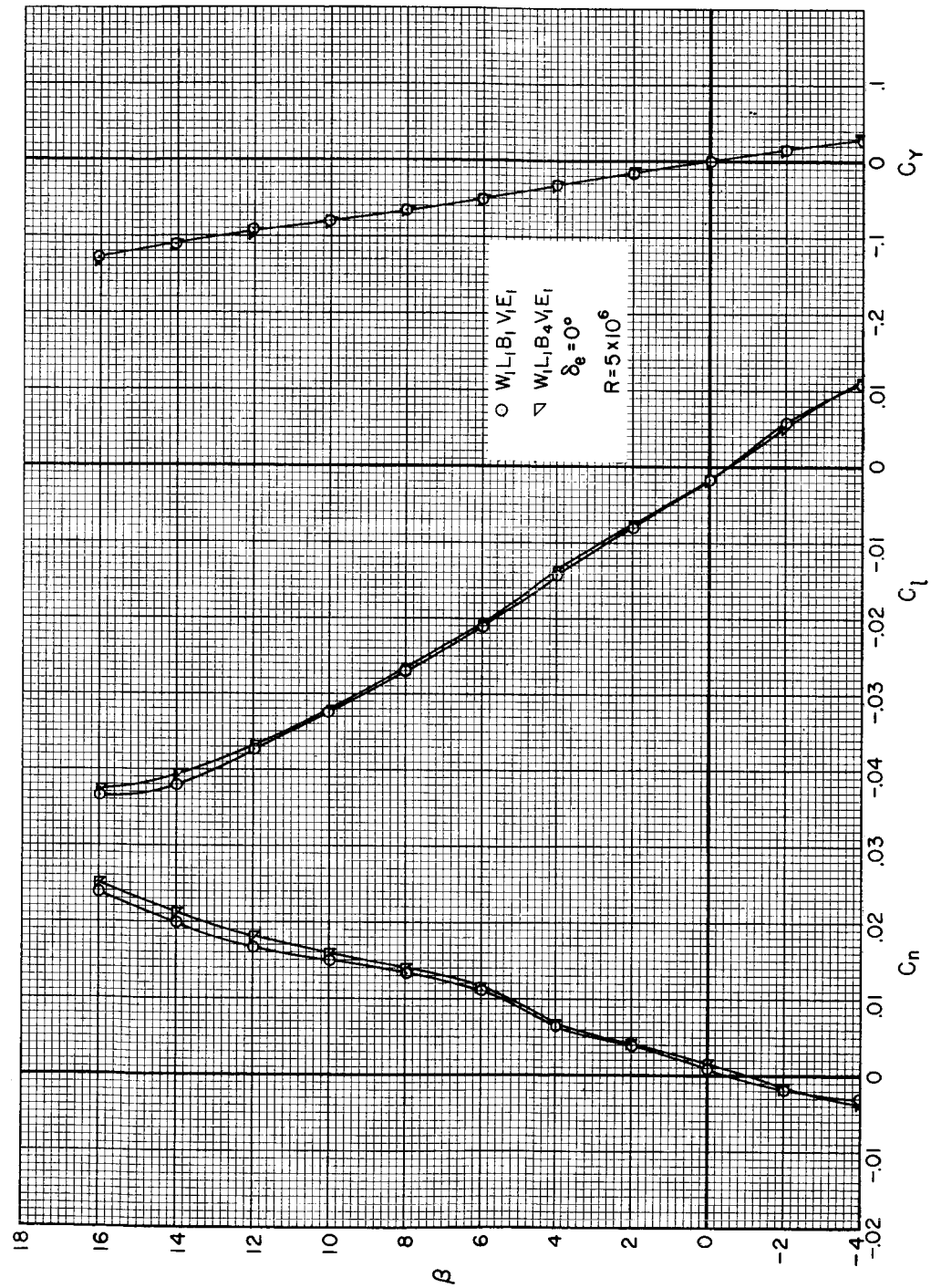

(c) $\alpha = 90°$

Figure 24.- Concluded.

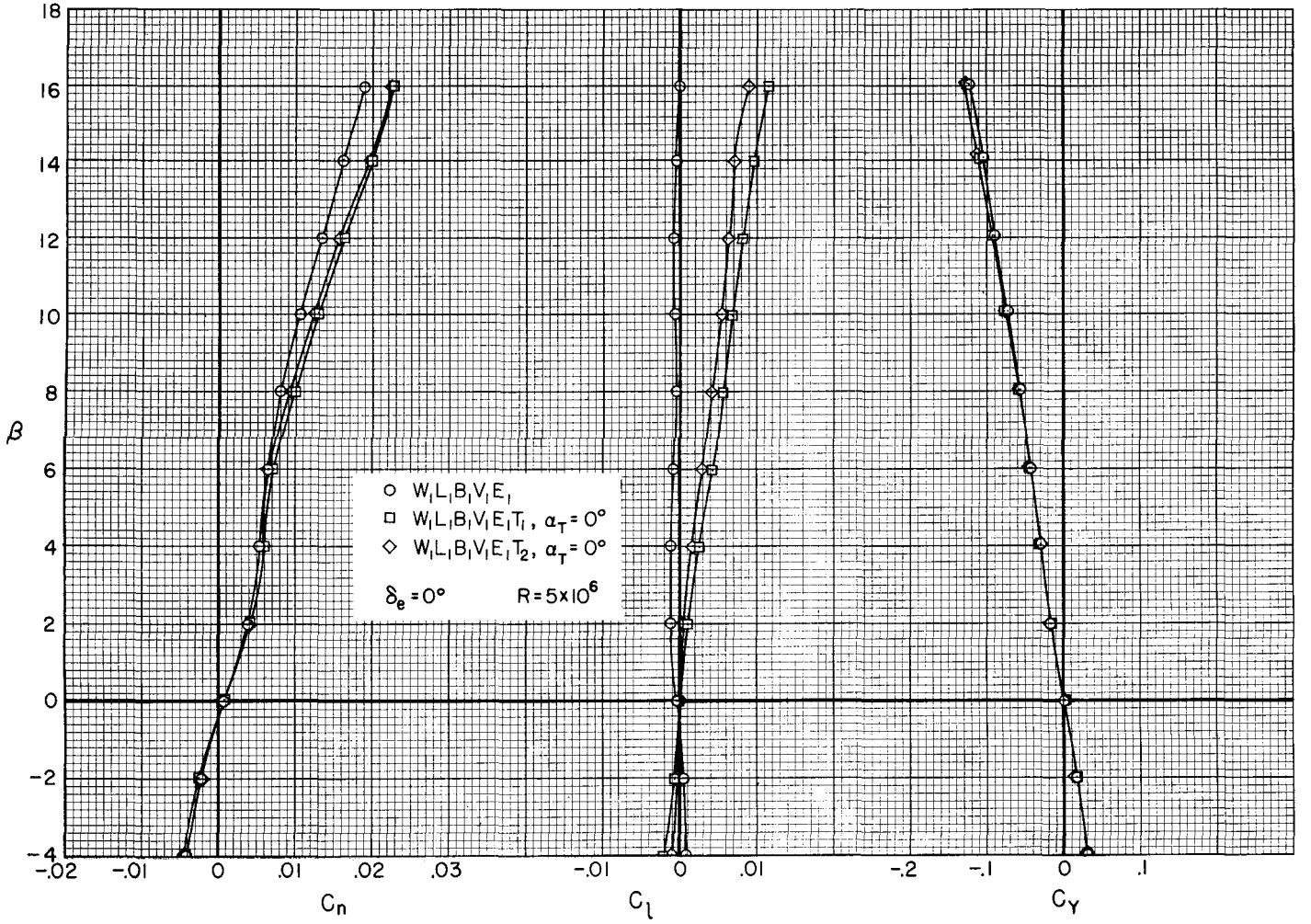

(a) $\alpha = 0^\circ$

Figure 25.- The effects of wing-tip extensions on the lateral-directional characteristics as functions of angle of sideslip; M = 0.26.

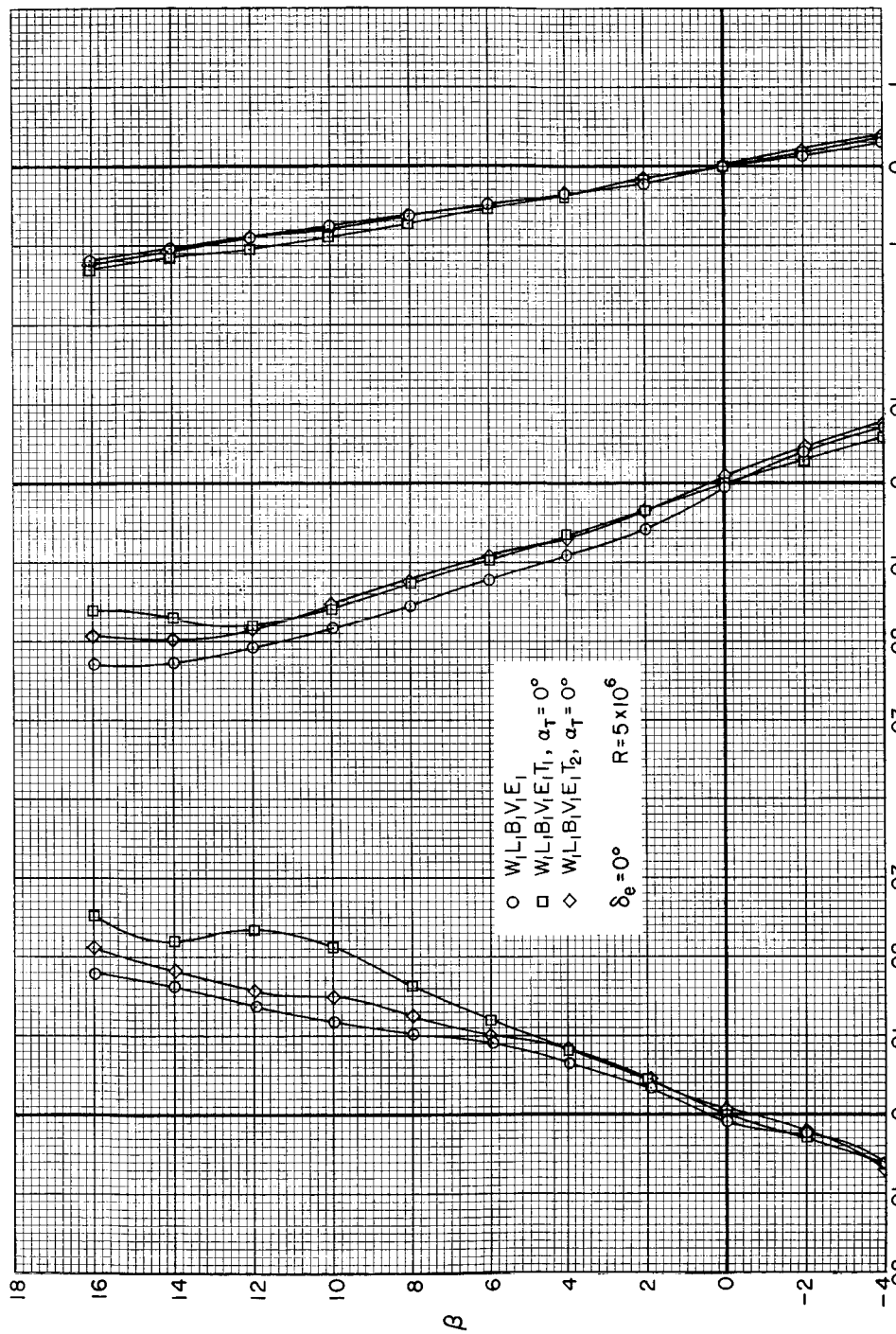

(b) $\alpha = 6°$

Figure 25.- Continued.

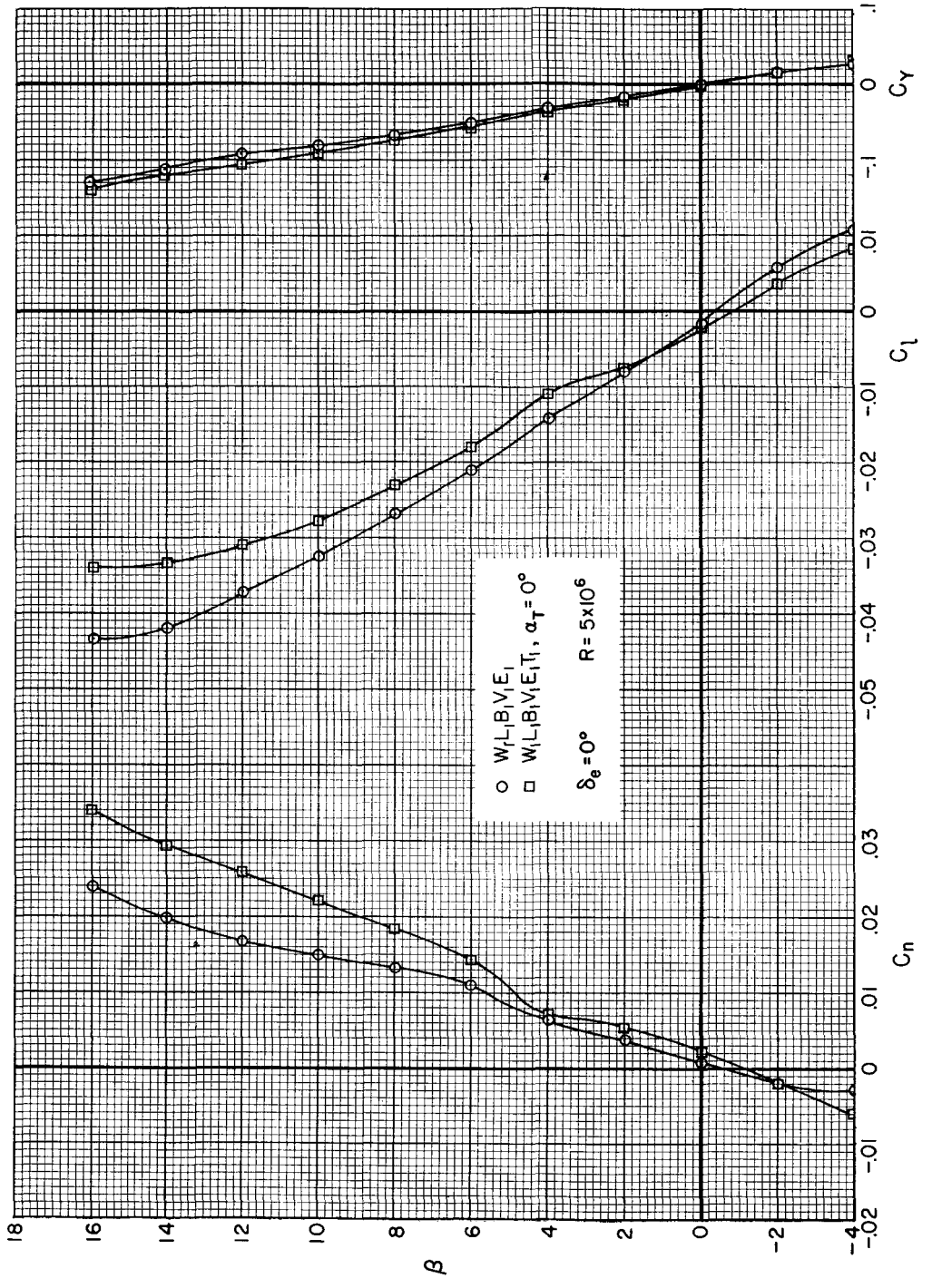

(c) $\alpha = 9°$

Figure 25.- Concluded.

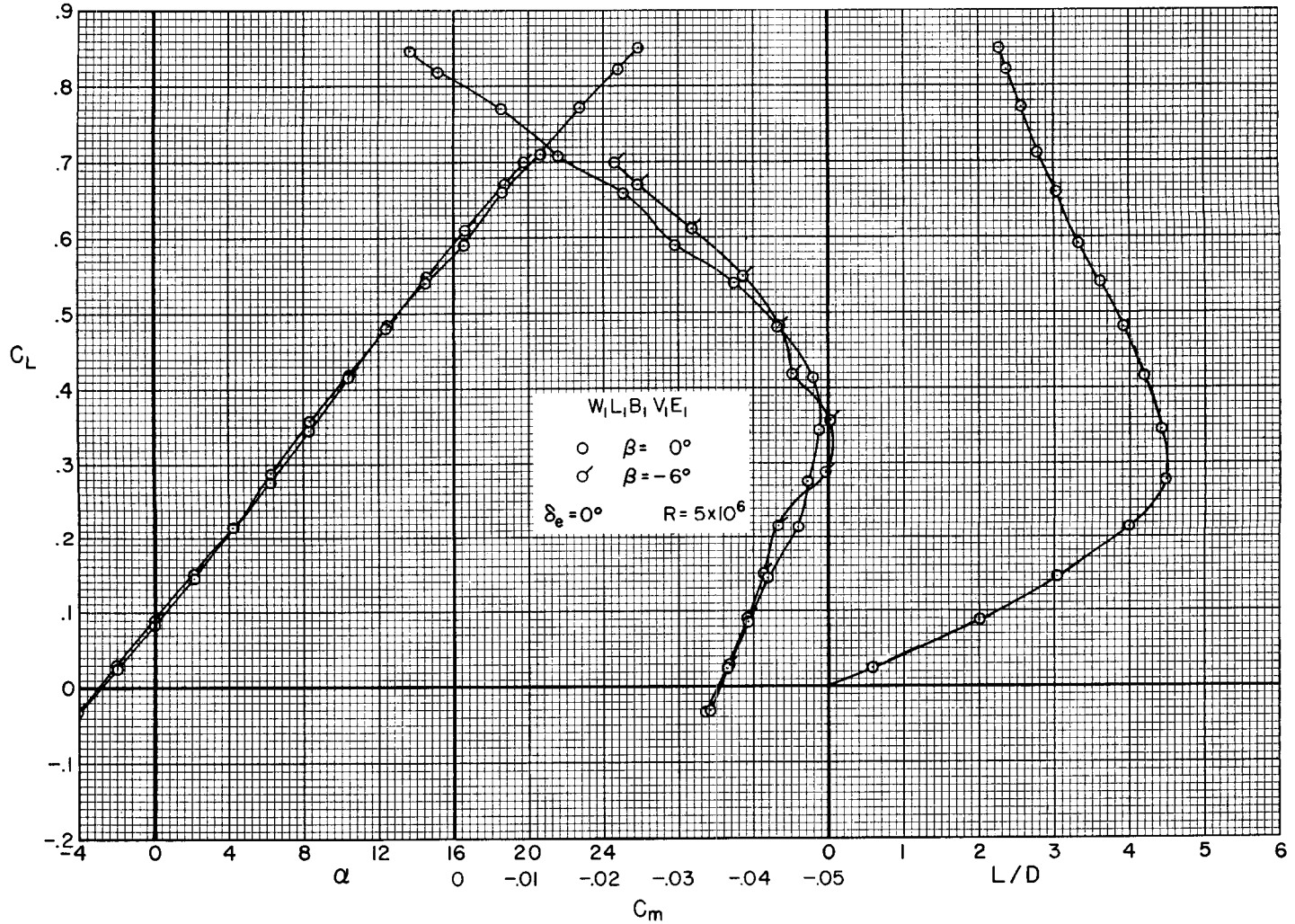

(a) C_L vs. α; C_L vs. C_m; C_L vs. L/D

Figure 26.- The effects of 6° sideslip on the aerodynamic characteristics; M = 0.26.

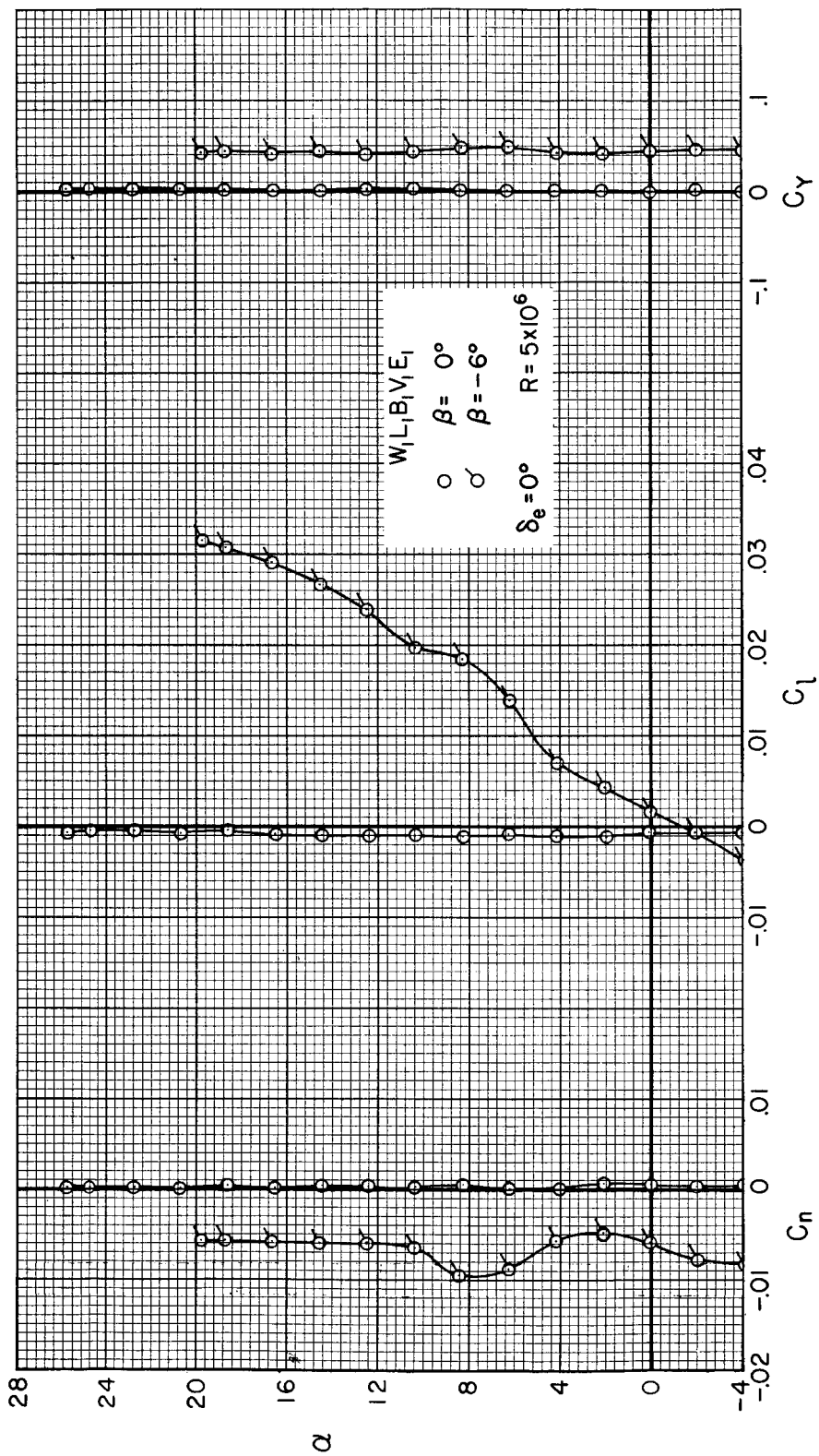

(b) C_n vs. α; C_l vs. α, C_Y vs. α

Figure 26.- Concluded.

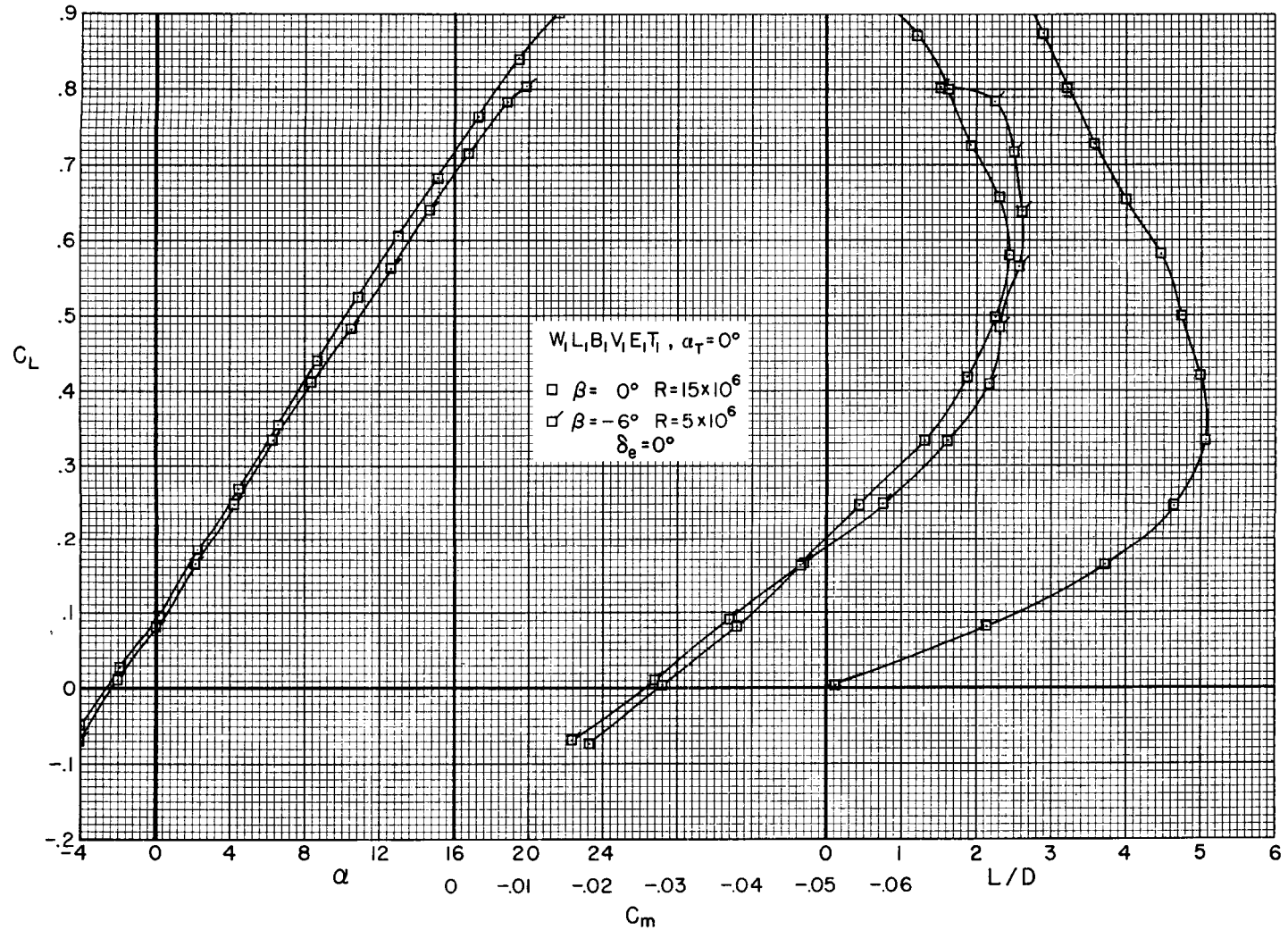

(a) C_L vs. α; C_L vs. C_m; C_L vs. L/D

Figure 27.- The effects of 6° sideslip on the aerodynamic characteristics with wing-tip extensions; M = 0.26.

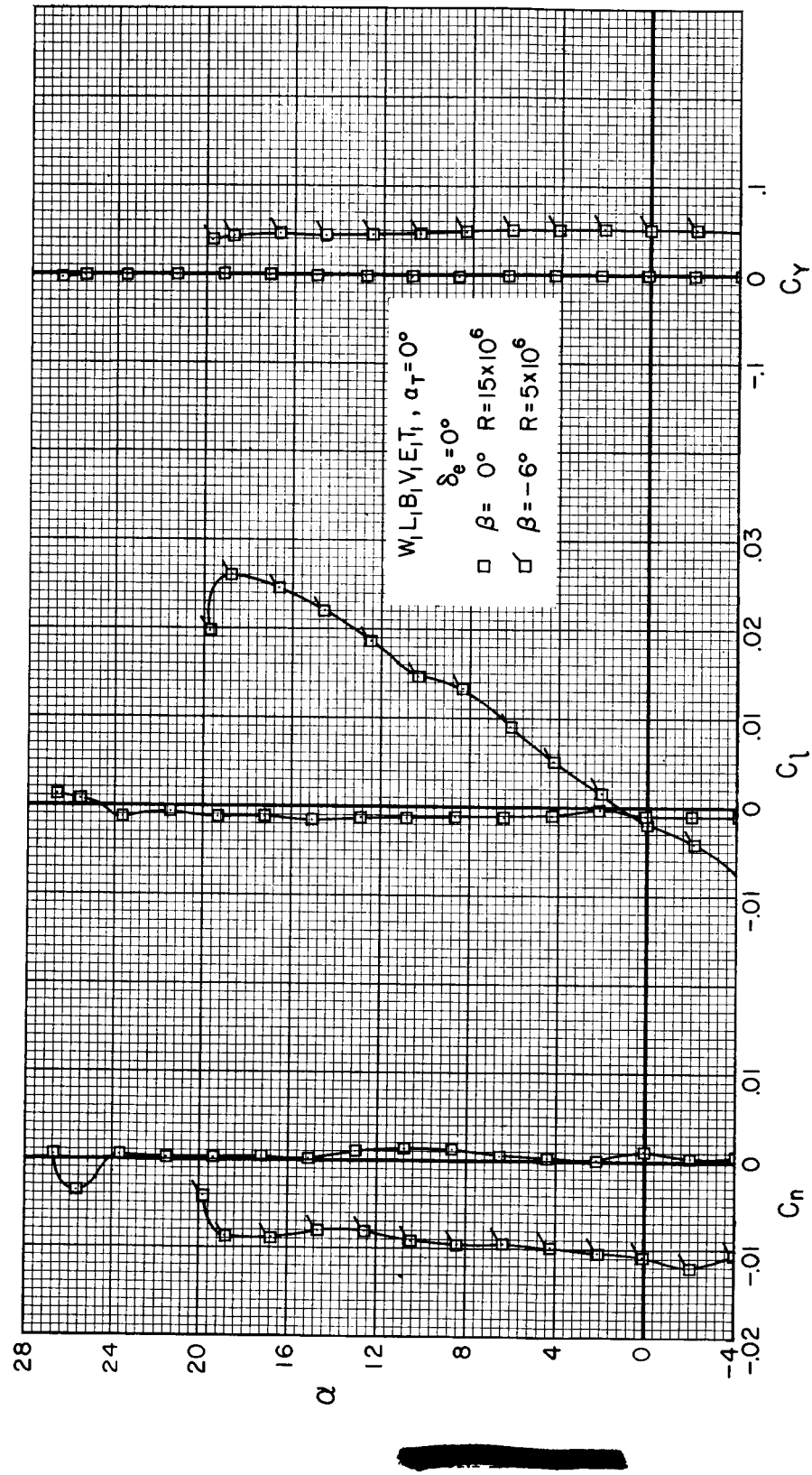

(b) C_n vs. α; C_l vs. α; C_Y vs. α

Figure 27.- Concluded.

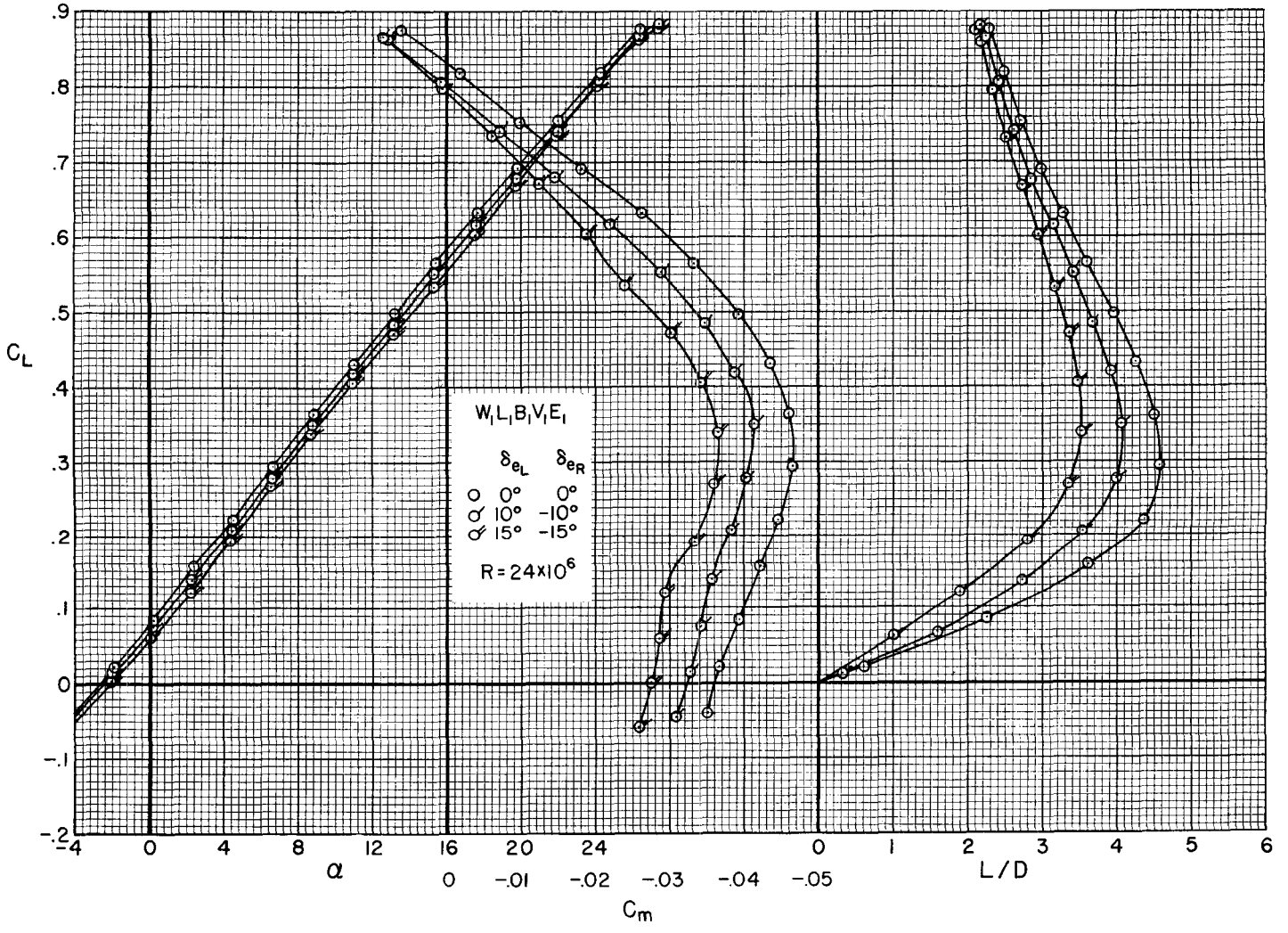

(a) C_L vs. α; C_L vs. C_m; C_L vs. L/D

Figure 28.- The effects of differential elevon deflection on the aerodynamic characteristics; $\beta = 0^o$, M = 0.26.

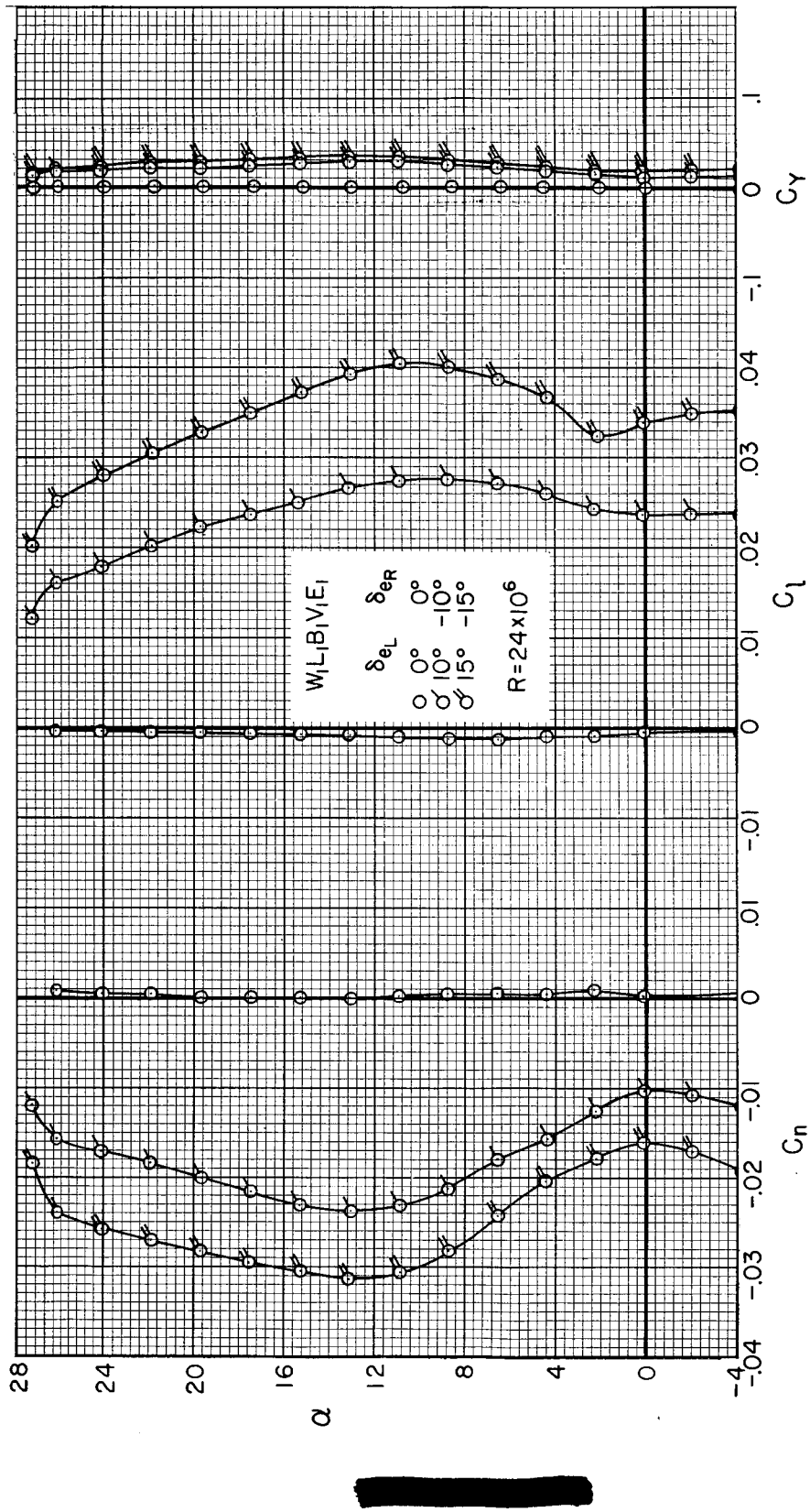

(b) C_n vs. α; C_l vs. α; C_Y vs. α

Figure 28.- Concluded.

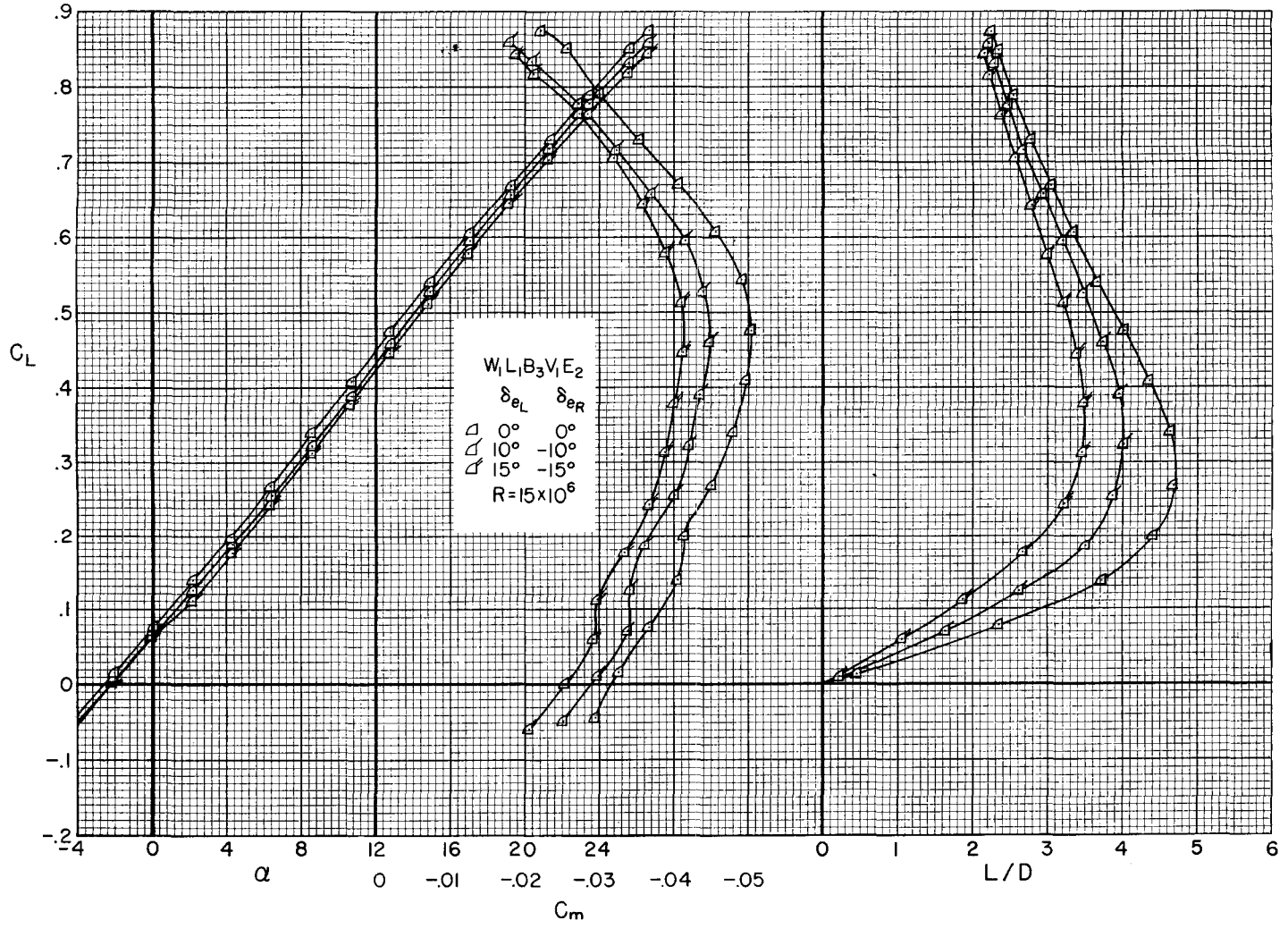

(a) C_L vs. α; C_L vs. C_m; C_L vs. L/D

Figure 29.- The effects of differential elevon deflections on the aerodynamic characteristics for large elevons, and extended body; $\beta = 0^o$, M = 0.26.

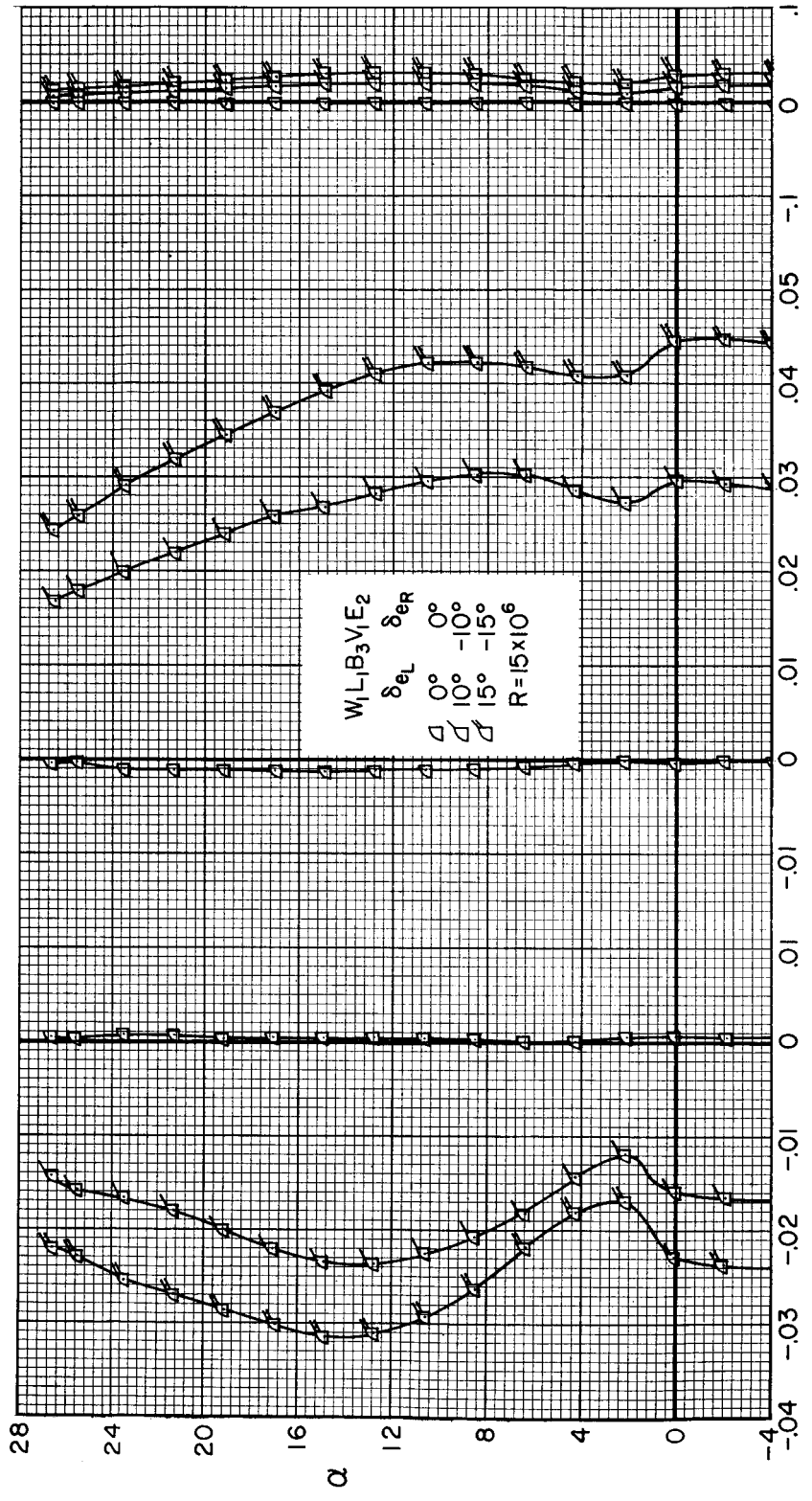

(b) C_n vs. α; C_l vs. α; C_Y vs. α

Figure 29.- Concluded.